

Electronic Thesis and Dissertation Repository

9-29-2020 12:30 PM

Some Insurance Options on Stochastic Drawdowns

Filip Dikic, *The University of Western Ontario*

Supervisor: Li, Shu, *The University of Western Ontario*

A thesis submitted in partial fulfillment of the requirements for the Master of Science degree in
Statistics and Actuarial Sciences

© Filip Dikic 2020

Follow this and additional works at: <https://ir.lib.uwo.ca/etd>

Recommended Citation

Dikic, Filip, "Some Insurance Options on Stochastic Drawdowns" (2020). *Electronic Thesis and Dissertation Repository*. 7377.

<https://ir.lib.uwo.ca/etd/7377>

This Dissertation/Thesis is brought to you for free and open access by Scholarship@Western. It has been accepted for inclusion in Electronic Thesis and Dissertation Repository by an authorized administrator of Scholarship@Western. For more information, please contact wlsadmin@uwo.ca.

Abstract

Insurance and options have been often used by investors to protect themselves from market crashes and significant financial losses. Thanks to its desired features, drawdowns can be a very useful tool in the marketplace, allowing investors to protect against the downside risks which commonly occur in the marketplace. Several insurance products are proposed via including protection against drawdown sizes, speed of market crash and frequency of drawdowns. We also design a knock-in drawdown option with generalized payoffs. In this thesis, we explore the probabilistic approach to drawdowns and use the technique of Laplace transform to find the fair market price of the designed insurances/options. Their connections with the existing models are discussed, and numerical results are then demonstrated as well as the sensitivity tests.

Keywords: Drawdown process, Laplace transform, Brownian motion, Spectrally negative Lévy process, Scale function, Valuation

Summary for Lay Audience

The financial market is a place where great gains and losses are created for investors every day. From the risk control's point view, investors could prevent themselves from the suffering of large losses on the financial products through the purchase of the insurances and options. The insurance provides a guarantee of compensation for specified losses, and an option helps limit the size of loss via its payoff design and in the strategy of hedging. Drawdown is one of the performance measures commonly used in the financial market, which determines the declines in value of the asset over time. With the help of drawdown measure, we could answer the questions like, how much the asset price has been dropped from its previous maximum value, how many days it takes for such a drop, and how many such drops occur in a year. Based on the size, speed and frequency of drawdowns, we design an insurance that provides the protection on the series of drawdown events. And an cheaper option is also proposed, whose strike price depends on the historical maximum given a drawdown event happens. The insurance and option are priced fairly using regular financial standards and advanced mathematical techniques. Finally, these newly proposed insurance and option are tested through various possible market variations, and we are able to connect them with the existing options in the marketplace.

Contents

Abstract	iii
Summary for Lay Audience	iv
List of Figures	vii
List of Tables	viii
List of Appendices	ix
1 Introduction	1
1.1 Related Studies	1
1.2 The drawdown process and drawdown-related quantities	3
1.3 Risk processes	5
1.3.1 One-Dimensional Linear Diffusion Model	6
1.3.2 Spectrally Negative Lévy process	7
1.4 Laplace Transform and its numerical inversion	7
1.5 Chapter Outline and Notations	11
2 Drawdown Insurance on the Frequency and Speed of Market Crash	13
2.1 Frequency of Drawdowns	13
2.2 Speed of Market Crash	15
2.3 Model setup	17
2.4 Preliminary results of drifted BM	18
2.5 The valuation of a drawdown insurance	20
2.5.1 Without recovery case	20
2.5.2 With recovery case	25
2.6 Numerical results on two-dimensional LT Inversion	26
3 Knock-in Options on the Size of Drawdown Risk	31
3.1 Model setup	31
3.2 Preliminary results	32
3.2.1 Spectrally negative Lévy process	32
3.2.2 Drifted BM	34
3.3 The valuation of knock-in drawdown options	35

3.4	Connections with the existing models	40
3.4.1	Connection with lookback put option	40
3.4.2	Connection with digital option on maximum drawdown	41
3.5	Numerical results	42
3.5.1	Type I option	42
3.5.2	Type II option	45
4	Conclusion and Future Work	49
	Bibliography	51
A	Proof of Equation (3.18)	53
B	Proof of Equation (3.20)	56
	Curriculum Vitae	58

List of Figures

2.1	Illustration of multiple drawdowns with recovery.	14
2.2	Illustration of multiple drawdowns without recovery.	14
2.3	Rising and crashing part of drawdowns illustrated here.	16
2.4	Sensitivity tests for $V(T, b)$ Contract I without recovery case	28
2.5	Sensitivity tests for $\tilde{V}(T, b)$ Contract I with recovery case	30
3.1	Sensitivity tests for Type I knock-in drawdown option $V_1(T)$	44
3.2	The values of $V_2^\beta(T)$ with black representing $\beta = 1$ and red representing $\beta = 0$.	46
3.3	Sensitivity tests for Type II knock-in drawdown option $V_2(T)$	47
3.4	Sensitivity test for Type II knock-in drawdown option $V_2(T)$ wrt a	48

List of Tables

1.1	The nine two-dimensional Laplace inversion algorithms	11
2.1	Numerical results for $V(T, b)$ Contract I without recovery case	27
2.2	Numerical results for $\tilde{V}(T, b)$ Contract I with recovery case	27
3.1	The fair market value of Type I knock-in drawdown option $V_1(T)$	43
3.2	Comparison of $V_1(T) _{a=0}$ with the lookback option	43
3.3	The fair market value of Type II knock-in drawdown option $V_2(T)$	45

List of Appendices

Appendix A Proof of Equation (3.18)	53
Appendix B Proof of Equation (3.20)	56

Chapter 1

Introduction

Ever since the industrial revolution at the start of the 20th century, the financial market and the economy have been hot topics in society. From the first major market crash known as The Great Depression in the 1930s to the recent financial crisis in 2007-2008, there have been not only studies and research done on attempting to reduce the impact of a crash but also helping to predict and prevent these market crashes. An important statistic that has recently come into practice in many areas is known as a drawdown. The drawdown is defined as the difference between the current value and the historical maximum value of a portfolio or underlying asset. Drawdowns provide a unique measure of risk as it gives us the drop in value as time goes. Drawdowns can be tracked in frequency, severity and speed, or how long the crash took to occur. With the combination of these features, many useful measures can be derived to capture not only the financial distress but also to help design new insurance products to protect against these adverse events. These products can be designed and tailored to protect against the frequency, severity and speed of drawdowns, and provide investors or companies with a new way to hedge against the market or risk management.

In this thesis, we consider the applications and practical uses of drawdowns as well as taking a theoretical approach to analyze the drawdown process. Beginning by looking at the first passage times of the underlying process and drawdown process and defining the probabilistic results, we go on to define several basic and some more complex drawdown insurance products. Though the use of Laplace transforms and Laplace inversion, we are able to provide mathematical analysis as well as determine explicit expressions for their fair market valuation. The insurance options that we proposed in this thesis provide protection for investors and traders on markets on the downside risk, and help hedge against significant losses in the market. Overall, this thesis covers only a few of all the possibilities that exist and the hope is to stimulate an environment in which other researchers and practitioners can continue to expand and further explore these products' feasibility in the real insurance market.

1.1 Related Studies

There have been many studies on the aspects of drawdowns and their applications. In probability, one such is the first passage time of the drawdown process derived in [16]. Furthermore, the probabilistic characteristics of the drawdown process under Brownian motion were studied in

[6] to determine probabilities and distribution of the process. Another interesting study by [14] focuses on the maximum drawdown captured, the associated risk and how it affects the price flow of an investment. The study provides applications of the maximum drawdown to maximum drawdown-at-risk, and classifying investment portfolios according to performance when controlling the losses via the maximum drawdown. Building on this maximum drawdown idea, there is also a modified performance measure known as Calmar ratio. This is similar to the well-known Sharpe ratio, however Calmar ratio is computed as the average annual rate of return divided by the maximum drawdown. Return Over Maximum Drawdown is another very similar performance measure, being that it is not average annual rate of return but instead just the actual return divided by maximum drawdown. Both measures are useful to measure performance in different aspects. For the Calmar ratio and more on maximum drawdown under Brownian motion see e.g., [13]. It is also of interest to consider the speed of market crash, i.e., how quickly a drawdown occurs from maximum to current time. A study was done by [2] involving the speed of crash for Lévy insurance risk process. In specific, they had interests in the distribution of drawdowns and Laplace transform for speed of the crash.

A recent book [18] provides a more systematic study on the probabilistic characterizations of drawdown process and its applications. As for the drawdown measures, they examined the drawdowns preceding drawups in a finite time horizon, the speed of market crashes, frequency drawdown, as well as occupation times related to drawdown. In the application side, they considered the fair premiums of drawdown insurance and optimal trading with a trailing stop strategy. These applications could be a useful tool in the financial risk management to protect investors from crashes like the 2008 market crash and 2020 pandemic market crash. The drawdown-related options mentioned in [18] are listed in Section 1.2.

We would also like to point out the similarity of drawdown and traditional ruin theory here. Consider the simple time value of ruin, as discussed by Hans U. Gerber in his paper "On the Time Value of Ruin" [7]. The concept of ruin or bankruptcy is in theory quite simple, and using a simple Compound Poisson surplus process as example,

$$X_t = x + ct - \sum_{i=1}^{N_t} \epsilon_i,$$

where the surplus is defined as X_t , x is the starting value, c the increasing coefficient based on time t and ϵ_i the i^{th} loss. Using this simple surplus process, we can map out a sample path and determine the probability of ruin or bankruptcy as an indicator of the surplus risk. As seen in [7], the (infinite) ruin concept is simply defined as the first time that the surplus level drops below level 0. They proposed the Gerber-Shiu penalty function and used it to discuss the joint distribution of the time of ruin with the surplus immediately before ruin and the deficit after ruin as a function of initial surplus values. The idea of ruin can be done in a finite time horizon, as seen in [5] where they considered both the finite and infinite ruin probabilities. Parisian ruin is another expansion on classical ruin theory, in which a grace period in the red zone is allowed, in other words, the Parisian ruin occurs when the surplus level remains in a dangerous level for a certain time period. In all these cases, the idea is about exit, where we consider the probability, time and severity when the surplus level (modeled by a stochastic process) exceeds from a certain barrier(s) of level (and time). This idea is consistent with the definition of drawdown, where the exit is considered when the surplus process drops below a

lower barrier from the historical maximum value. In this case, the lower barrier is changing throughout time as the maximum of the process changes (which is non-decreasing). Along this line, recently a general drawdown is proposed, which include the traditional drawdown and ruin as special cases. Also [10] and [11] considered drawdown as a risk indicator in the surplus process that provides the timely warnings to the insurer before a capital shortfall, and they discussed the regime-switching model based on drawdown risk and how this strategy outperformed its counterparts in either single regime strategy.

1.2 The drawdown process and drawdown-related quantities

To provide a sufficient introduction and provide a solid foundation to the work done in this thesis, we begin by covering the basics and introducing previous results and research done on the area of drawdowns. A drawdown can be traditionally defined as the difference between the present value of an asset defined as X_t and the running maximum of that process at some time t , and this can be written explicitly as

$$D_t := \bar{X}_t - X_t, \quad (1.1)$$

where the running maximum at time t is

$$\bar{X}_t := \sup_{s \in [0, t]} X_s. \quad (1.2)$$

Another potential useful and informative statistic can be the drawup. This can be used in similar ideas as the drawdown, but rather than recording drops in an asset value, it can be used to record increases. In the case of a drawup, we need the current process of an asset X_t , the running minimum of the process, and drawup process is defined as

$$U_t := X_t - \underline{X}_t, \quad (1.3)$$

where the running minimum

$$\underline{X}_t := \inf_{s \in [0, t]} X_s. \quad (1.4)$$

While measuring single drawdowns already has many applications, measuring drawdowns of certain sizes and creating insurance to protect against drawdowns in the market, we can also expand the idea further by looking at the maximum of all drawdowns recorded in a process. For some maturity time T , at the current time t we can define the running maximum of the drawdown process as

$$\bar{D}_t := \sup_{s \in [0, t]} D_s. \quad (1.5)$$

The maximum of the drawdown process as be applied to the stock market and portfolios of investors to record the worst performance periods and to help determine overall periods of loss. Comparisons between portfolios can be made with each drawdown and the maximum drawdown process to determine the performance, such as the S&P 500. To provide further

insight, you can also look at the time of when each drawdown occurs of a specified size. In this case, if you are tracking a stock you are able to determine whether the drawdowns match with market recessions and determine how your portfolio and other stock perform. The concept of basic drawdowns, time of drawdowns as well as how long the market can take to crash from the maximum will be covered further in Chapter 2. These quantities defined here are meant to be an introduction to the most basic definition of drawdowns and show all the possibilities and applications that exist within the drawdown framework. The first drawdown time can be seen as the first passage time of the drawdown process, meaning the time taken for the drawdown process to reach a certain variable. In the most simple case, we can assume for some $a > 0$, that a is that prespecified threshold in which our stopping time can be defined as

$$\tau_D^+(a) := \inf\{t > 0 : D_t > a\}, \quad (1.6)$$

which is the time of the first drawdown. The probabilistic approach using Laplace transforms can be used to determine the density of the first drawdown time, as well as other useful variables. Further drawdown process properties and variables will be discussed and explained in the latter chapters — specifically Chapter 2. Rather than only considering the drawdown process, we can also consider the stochastic process $\{X_t\}_{t \geq 0}$ with first passage times defined as

$$\tau_X^+(a) := \inf\{t > 0 : X_t > a\}, \quad (1.7)$$

$$\tau_X^-(a) := \inf\{t > 0 : X_t < a\}. \quad (1.8)$$

Another interesting and well known application that can be applied to drawdowns is the two-sided exit problems, such as those under the Lévy processes. In such case, we consider the previous first passage times and compare the two times to determine the probability that some process $X_0 = x$ in $y < x < z$ will reach y or z first, before a maturity time T . The objective with the two-sided exit problem is to obtain the Laplace transform of the density of the function, or in this case the process. As such, we can define the two-sided exit problems as

$$\mathbb{E}_x(e^{-q\tau_X^-(y)} \mathbf{1}_{\{\tau_X^-(y) < \tau_X^+(z)\}}) = \mathbb{P}_x(\tau_X^-(y) < \tau_X^+(z) \wedge T), \quad (1.9)$$

$$\mathbb{E}_x(e^{-q\tau_X^+(z)} \mathbf{1}_{\{\tau_X^+(z) < \tau_X^-(y)\}}) = \mathbb{P}_x(\tau_X^+(z) < \tau_X^-(y) \wedge T). \quad (1.10)$$

where T is our maturity time. In some cases, through the process of Canadization, we can Canadize T letting $T = e_q$ be an exponentially distributed variable with parameter $q > 0$.

Previously, we mentioned many different drawdown related products such as those protecting against speed of market crash and multiple drawdowns occurring. The list shown below gives an idea of just some of the possibilities of the variety in insurance contracts and how investors can protect themselves in different ways in the market. The full list, which are products from [18], is given as:

- Speed of Market Crash Option: $V_B(K) = \mathbb{E}^{\mathbb{Q}}(e^{-r\tau_D^+(a)} \cdot \mathbf{1}_{\{S_a < K, X_{ga} < B\}})$,
 - Claim pays \$1 at $\tau_D^+(a)$ if the underlying process has not been knocked out by the drawdown time and the speed of market crash is smaller than a strike K .

- Multiple Drawdowns Insurance Option No. 1: $V_1(T) = e^{-rT} \mathbb{E}^{\mathbb{Q}}(N_T^a(X))$,
 - Claim pays \$k at maturity time T if a total of k drawdowns (without recovery, in this example) over the size a occurred prior to T . The $N_T^a(X)$ is the count of the number of drawdowns that occurred.
- Multiple Drawdowns Insurance Option No. 2: $V_2(T) = \sum_{k=1}^{\infty} \mathbb{E}^{\mathbb{Q}}(e^{-r\tau_D^{k,+}(a)} \cdot 1_{\{\tau_D^{k,+}(a) \leq T\}})$,
 - As above, this claim is the same but rather than paying \$k at maturity time T , it pays \$1 at each of the k drawdowns.
- Parisian-like Digital Call Option: $P_0(a, K, T) = e^{-rT} \mathbb{Q}\left(\int_0^T 1_{\{D_t > a\}} dt > K\right)$,
 - The market is assumed to be complete, and so \mathbb{Q} is the risk-neutral measure. This Parisian-like digital call option pays \$1 if the drawdown exceeds a for some time period of strike K before the maturity time $T > 0$.
- Digital Call on Maximum Drawdown: $DC_t^{\bar{D}}(K, T) := e^{-r(T-t)} \mathbb{Q}_t^T(\bar{D}_T \geq K)$,
 - The value of the call at time $t \in [0, T]$ for some maturity time T . Pays \$1 if the maximum drawdown exceeds some strike K .
- Digital Call on K-DD Preceding K-DU: $DC_t^{D < U}(a, T) := e^{-r(T-t)} \mathbb{Q}_t^T(\tau_D^+(a) \leq \tau_U^+(a) \wedge T)$,
 - Just as the previous option, the price is at some time $t \in [0, T]$ for some maturity time T . Payment of \$1 if a drawdown of size a occurs before a drawup of the same size and before maturity time T .
- One touch Knockout Option: $OTKO_t(V, W, T) := e^{-r(T-t)} \mathbb{Q}_t^T(\tau_s^-(V) \leq T, \bar{S}_{\tau_s^-(V)} < W)$,
 - This option pays \$1 at the maturity time T if and only if the spot price S_t hits the in-barrier V before hitting the out-barrier W and before maturity time T .
- Ricochet Up-First Down-and-in: $RUFDI_t(V, W, T) = e^{-r(T-t)} \mathbb{E}_t^{\mathbb{Q}}(1_{\{\tau_s^-(V) \leq T\}} \delta(\bar{S}_{\tau_s^-(V)} - W))$.
 - Similar to the above option, this option is a sequential double-touch as the payoff is the result of differentiating the payoff of the one-touch option with respect to W . In this case, a positive payoff occurs if the underlying S_t touches W and then hits V from above before the maturity time T .

In the above contracts, r is the risk-free rate and all the valuation is done under the risk-neutral measure \mathbb{Q} .

1.3 Risk processes

This section will introduce two risk processes, namely one-dimensional linear diffusion model and spectrally negative Lévy model. Details of their properties, including their scale function, two-sided exit problem and so on will be presented. These results will be used in the following chapters. Note that drifted Brownian motion model is a special case of both the linear diffusion process and the spectrally negative Lévy process.

1.3.1 One-Dimensional Linear Diffusion Model

Consider a one-dimensional linear diffusion process $X = \{X_t\}_{t \geq 0}$ on $I \equiv (l, r) \subset \mathbb{R}$. The infinitesimal generator is given as

$$\mathcal{L} = \frac{1}{2}\sigma^2(x)\frac{\partial^2}{\partial x^2} + \mu(x)\frac{\partial}{\partial x}, \quad (1.11)$$

where $(\mu(\cdot), \sigma(\cdot))$ is a pair of real-valued functions on I such that

$$\sigma^2(x) > 0, \forall x \in I,$$

$$\forall x \in I, \exists \epsilon > 0 \text{ such that } \int_{x-\epsilon}^{x+\epsilon} \frac{1 + |\mu(y)|}{\sigma^2(y)} dy < \infty.$$

The scale function $s(\cdot)$ associated with the linear diffusion process is an increasing function from I to \mathbb{R} , such that $(\mathcal{L}_X s)(x) = 0$ for all $x \in I$. The particular scale function can be chosen as

$$s'(x) = \exp\left(-\int_{\mathcal{K}'}^x 2\mu(y)/\sigma^2(y)dy\right),$$

for some fixed $\mathcal{K}' \in I$. From Appendix A of [18], a well-known result of the Laplace transforms of the first passage times $\tau_{\mathcal{K}}^{\pm}(y)$ gives two independent solutions to the Sturm-Liouville equation $\mathcal{L}f(x) = qf(x)$. The results are specifically given for $x, \mathcal{K} \in I$ as

$$\phi_q^+(x) := \begin{cases} \mathbb{E}_x(e^{-q\tau_{\mathcal{K}}^+(x)}) & x \leq \mathcal{K}, \\ \frac{1}{\mathbb{E}_{\mathcal{K}}(e^{-q\tau_{\mathcal{K}}^+(x)})} & x > \mathcal{K}, \end{cases}$$

$$\phi_q^-(x) := \begin{cases} \frac{1}{\mathbb{E}_{\mathcal{K}}(e^{-q\tau_{\mathcal{K}}^-(x)})} & x \leq \mathcal{K}, \\ \mathbb{E}_x(e^{-q\tau_{\mathcal{K}}^-(x)}) & x > \mathcal{K}. \end{cases}$$

Using the scale function $s(\cdot)$ from earlier, then there is a constant $w_q > 0$ which satisfies the following equation,

$$w_q \cdot s'(x) = \phi_q^{+'}(x)\phi_q^-(x) - \phi_q^{-'}(x)\phi_q^+(x). \quad (1.12)$$

Thus, one can further define the following functions $W_q(x, y), W_{q,1}(x, y)$ associated with the one-dimensional linear diffusion model as

$$W_q(x, y) = w_q^{-1} \left(\phi_q^+(x)\phi_q^-(y) - \phi_q^-(x)\phi_q^+(y) \right), \quad (1.13)$$

and

$$W_{q,1}(x, y) = \frac{\frac{\partial}{\partial x} W_q(x, y)}{W_q(x, y)}. \quad (1.14)$$

For $y < x < z$ and $q \geq 0$, we have

$$\mathbb{E}_x(e^{-q\tau_{\mathcal{K}}^+(y)} \cdot \mathbf{1}_{\{\tau_{\mathcal{K}}^+(y) < \tau_{\mathcal{K}}^-(z)\}}) = \frac{W_q(x, z)}{W_q(y, z)},$$

and

$$\mathbb{E}_x(e^{-q\tau_{\mathcal{K}}^-(z)} \cdot \mathbf{1}_{\{\tau_{\mathcal{K}}^-(z) < \tau_{\mathcal{K}}^+(y)\}}) = \frac{W_q(y, z)}{W_q(y, z)}.$$

1.3.2 Spectrally Negative Lévy process

The next model used is the Spectrally Negative Lévy process. Consider a one-dimensional Lévy process $X = \{X_t\}_{t \geq 0}$ defined on a filtered probability space $(\Omega, \mathbb{F}, \mathcal{F}, \mathbb{P})$ with filtration $\mathbb{F} = \{\mathcal{F}_t\}_{t \geq 0}$. We can consider the Laplace exponent of this X , as:

$$\psi(s) = \log \mathbb{E}(e^{sX_1}) = -\mu s + \frac{\sigma^2}{2} s^2 + \int_{(-\infty, 0)} (e^{sx} - 1 - sx \mathbf{1}_{\{x > -1\}}) \Pi(dx) \quad (1.15)$$

for every $s \in \mathbf{H}_{\geq 0} = \{s \in \mathbf{C} : \Re(s) \geq 0\}$. In this Laplace exponent, we have $\sigma \geq 0$ and the Lévy measure $\Pi(dx)$ is supported on $(-\infty, 0)$ with

$$\int_{(-\infty, 0)} (1 \wedge x^2) \Pi(dx) < \infty.$$

The previous Laplace exponent formula $\psi(s)$ has at least one positive solution $q, q \geq 0$ and the largest of these solutions is denoted by $\Phi(q)$, i.e.,

$$\Phi(q) = \sup\{\lambda : \psi(\lambda) = q\}.$$

As a special case of the spectrally negative Lévy process, Brownian motion with drift is a Lévy process with no jumps and Laplace exponent for X , given as $\psi(s) = \frac{\sigma^2}{2} s^2 + \mu s$, where σ is the diffusion coefficient and μ is the drift. The right inverse of the Laplace exponent is $\Phi(q) = -\frac{\mu}{\sigma^2} + \sqrt{\left(\frac{\mu}{\sigma^2}\right)^2 + \frac{2q}{\sigma^2}}$.

Under the spectrally negative Lévy process X with Laplace exponent ψ , we can define a family of functions indexed by $q \geq 0, W^{(q)} : \mathbf{R} \rightarrow [0, \infty)$. For each given $q \geq 0$, we have $W^{(q)}(x) = 0$ when $x < 0$ and otherwise on $[0, \infty)$ is a unique right continuous function. The Laplace transform of this is given by:

$$\int_0^\infty e^{-sx} W^{(q)}(x) dx = \frac{1}{\psi(s) - q}. \quad (1.16)$$

There are two well known fluctuation identities of spectrally negative Lévy processes from [8] provided in [18]. For $q \geq 0$ and $0 \leq x \leq a$, we have the following results:

$$\mathbb{E}_x(e^{-q\tau_x^+(a)} \cdot \mathbf{1}_{\{\tau_x^+(a) < \tau_x^-(0)\}}) = \frac{W^{(q)}(x)}{W^{(q)}(a)}, \quad (1.17)$$

and

$$\mathbb{E}_x(e^{-q\tau_x^-(0)} \cdot \mathbf{1}_{\{\tau_x^-(0) < \tau_x^+(a)\}}) = Z^{(q)}(x) - Z^{(q)}(a) \frac{W^{(q)}(x)}{W^{(q)}(a)}, \quad (1.18)$$

where $Z^{(q)}(x) = 1 + q \int_0^x W^{(q)}(y) dy$.

1.4 Laplace Transform and its numerical inversion

A main technique that we use in the subsequent sections is the Laplace Transform (LT). Laplace transforms are very useful in many applications such as solving differential equations.

A Laplace transform is an integral transform of a function $f(t)$, defined for all real numbers $t \geq 0$, as such

$$\tilde{f}(s) = \int_0^{\infty} e^{-st} f(t) dt, \quad (1.19)$$

where s is the Laplace argument. For example, the LT of exponential density $f(t) = \mu e^{-\mu t}$ is

$$\tilde{f}(s) = \int_0^{\infty} e^{-st} f(t) dt = \frac{\mu}{\mu + s}.$$

A two-dimensional LT is defined for a bi-variate function $f(x, y)$, $x, y \geq 0$,

$$\tilde{f}(s, r) = \int_0^{\infty} \int_0^{\infty} e^{-sx} e^{-ry} f(x, y) dx dy,$$

where s (or r) is the Laplace argument with respect to variable x (or y). Similarly one can generalize the definition of LT to multiple dimension.

An important property of LT is its one-to-one mapping from the original function to its transformation function. If a LT has the form $\tilde{f}(s) = \frac{\mu}{\mu + s}$, we know immediately that the LT inversion yields $f(t) = \mu e^{-\mu t}$.

However, some LTs might be of complicated forms, whose inverse transform can not be obtained directly. In these cases, we need to rely on the algorithms to invert Laplace transforms numerically. For example in our case, to allow us to compute the price of these products using our probabilistic approach. However we cannot price the product using the Laplace transform as it contains the complex variable q , so we must perform the Laplace transform inversion to determine the real price. As mentioned before we are using a numerical Laplace transform inversion as the complexity of the payoff function in Laplace transform is too complex to do a simple inversion. Hence, in the following, we list the existing numerical LT inversion approaches from [1] for both one-dimensional and two-dimensional cases.

The framework used for numerical Laplace inversion is the approximation by a finite linear combination of the transform values using the inversion formula

$$f(t) \approx f_n(t) \equiv \frac{1}{t} \sum_{k=0}^n \omega_k \tilde{f}\left(\frac{\alpha_k}{t}\right), \quad 0 < t < \infty, \quad (1.20)$$

where ω_k are the weights and α_k are complex number nodes which depend on n . In each algorithm, this number n will be specified as some variety of $n = cM - a$ transformations, where c and a are chosen constants. This framework is especially useful as it has generalized nodes and weights which remain to be specified, thus allowing the use of many different algorithms. There are three specific algorithms discussed in [1] regarding to this numerical Laplace inversion: the Gaver-Stehfest algorithm (\mathcal{G}), the Euler summation (\mathcal{E}) and the Talbot algorithm (\mathcal{T}).

To better understand how this Laplace inversion works, specifically with each algorithm, we will look briefly into each model in the following. Firstly, the Gaver-Stehfest algorithm (\mathcal{G}) is the simplest of the three algorithms and fits directly into the desired framework as all weights and nodes are real numbers and do not have complex components. The Gaver-Stehfest

procedure is based on the sequence of Gaver approximants, and the Gaver-Stehfest inversion formula is given as

$$\mathcal{G}(M) := f_g(t, M) = \frac{\ln(2)}{t} \sum_{k=1}^{2M} e_k \tilde{f}\left(\frac{k \ln(2)}{t}\right), \quad (1.21)$$

where

$$e_k = (-1)^{M+k} \sum_{j=\lfloor (k+1)/2 \rfloor}^{k \wedge M} \frac{j^{M+1}}{M!} \binom{M}{j} \binom{2j}{j} \binom{j}{k-j},$$

and $\lfloor x \rfloor$ is the floor function of x , and $k \wedge M = \min\{k, M\}$. While $\mathcal{G}(M)$ has the benefit of simplicity, as it does not contain any complex numbers, it also has the lowest efficiency rating out of the three algorithms $eff(\mathcal{G}) \approx 0.4$, as well as takes the longest time to compute per M transformations. Efficiency rating is defined as

$$eff(\mathcal{G}) \equiv \frac{\text{significant digits produced}}{\text{precision required}}.$$

Under \mathcal{G} -algorithm, to obtain j significant digits then we let the number of transformations M be the $\lceil 1.1j \rceil$, where $\lceil x \rceil$ is the ceiling function of x .

The Euler algorithm (\mathcal{E}) is an implementation of the Fourier-series method, which has the following Euler inversion formula as

$$\mathcal{E}(M) := f_e(t, M) = \frac{10^{M/3}}{t} \sum_{k=0}^{2M} \eta_k \operatorname{Re} \left(\tilde{f}\left(\frac{\beta_k}{t}\right) \right), \quad (1.22)$$

where

$$\beta_k = \frac{M \ln(10)}{3} + \pi i k, \quad \eta_k = (-1)^k \epsilon_k,$$

with $i = \sqrt{-1}$ and

$$\epsilon_0 = \frac{1}{2}, \quad \epsilon_k = 1, 1 \leq k \leq M, \quad \epsilon_{2M} = \frac{1}{2M},$$

$$\epsilon_{2M-k} = \epsilon_{2M-k+1} + 2^{-M} \binom{M}{k}, \quad 0 < k < M.$$

This formula fits into the original framework designed for numerical Laplace inversion in Equation (1.20) with specified parameters for weights and nodes being given as $\omega_k = 10^{M/3} \eta_k$, $\alpha_k = \beta_k$ and $n = M$. Similarly to the \mathcal{G} -algorithm, about half of the terms in the Euler inversion formula are used to speed up convergence while using Euler summation. but the \mathcal{E} -algorithm tends to be more efficient. Actually the efficiency for the Euler algorithm is $eff(\mathcal{E}) \approx 0.6$, which is about 50% more than that of the \mathcal{G} -algorithm. To obtain j significant digits with the \mathcal{E} -algorithm, let M be the positive integer $\lceil 1.7j \rceil$.

The last algorithm is called Talbot algorithm, which also fits into the framework as it begins from the Bromwich integral. The Talbot inversion formula is given as

$$\mathcal{T}(M) := f_b(t, M) = \frac{2}{5t} \sum_{k=0}^{M-1} \operatorname{Re} \left(\gamma_k \tilde{f}\left(\frac{\delta_k}{t}\right) \right), \quad (1.23)$$

where

$$\delta_0 = \frac{2M}{5}, \quad \delta_k = \frac{2k\pi}{5}(\cot(k\pi/M) + i), \quad 0 < k < M,$$

$$\gamma_0 = \frac{1}{2}e^{\delta_0}, \quad \gamma_k = [1 + i(k\pi/M)(1 + [\cot(k\pi/M)]^2) - i \cot(k\pi/M)]e^{\delta_k}, \quad 0 < k < M,$$

with $i = \sqrt{-1}$. The weights and nodes in Equation (1.20) are defined respectively as $\omega_k = (2/5)\gamma_k$, $\alpha_k = \delta_k$ and $n = M$. In the \mathcal{T} -algorithm, both the weights and nodes are complex. The spacing between nodes is uneven. As well, the weights do not sum up to zero in the \mathcal{T} -algorithm but rather a very small sum

$$Re\left\{\sum_{k=0}^{M-1} \gamma_k\right\} \approx 10^{-0.6M}.$$

The efficiency of the \mathcal{T} -algorithm is about the same as the \mathcal{E} -algorithm, that is $eff(\mathcal{T}) \approx 0.6$. If j significant digits are required, then we let M be $\lceil 1.7j \rceil$.

In the case of two-dimensional numerical Laplace inversion, we are able to combine the three one-dimensional algorithms listed here in any order to create nine unique two-dimensional algorithms. Due to the combination of two one-dimensional algorithms, each two-dimensional algorithm has its own unique properties, and the order of combination matters. For example, the Talbot-Euler algorithm ($\mathcal{T}(M)\mathcal{E}(M)$) differs from the Euler-Talbot algorithm ($\mathcal{E}(M)\mathcal{T}(M)$). This is for several reasons. The first is the fact that when we combine two to create a two-dimensional algorithm, we now have two loops, where the weights and nodes in the outer loop are now dependent on the parameter M , while the weights and nodes in the inner loop depend on the parameter cM , where c is specified based on experience with collections of good transforms. Also, some algorithms involves the complex conjugates that do not appear in one-dimensional algorithms. Table 1.1 presents the nine two-dimensional formulas given in [1], as the combinations of the three one-dimensional Laplace inversion formula.

Three of the nine two-dimensional numerical inversion formulas contain a $c \neq 1$, as can be seen in their combination name (i.e. $\mathcal{G}(M)\mathcal{T}(3M)$ has $c = 3$ for the Talbot algorithm). These that are different have a prime symbol (seen as ') which identifies that the number of weights or nodes is different from the original algorithm as a result of the new number of transformations. From the performance analysis provided in [1], it can be seen that $\mathcal{T}(M)\mathcal{G}(M)$, $\mathcal{T}(M)\mathcal{T}(M)$ and $\mathcal{E}(M)\mathcal{G}(M)$ are amongst the fastest regarding execution time with lower number of transformations ($M = 10, M = 20$). With higher transformations, either combination of $\mathcal{T}(M)$ and $\mathcal{G}(M)$ perform very quickly, while $\mathcal{G}(M)\mathcal{E}(3M)$ has the slowest execution time in every M value tested. However, $\mathcal{G}(M)\mathcal{E}(3M)$ also provides the highest number of significant digits for almost each number of transformations M , therefore it can be seen as the most accurate. In any sense, several functions provide both accurate, efficient and quick results such as $\mathcal{T}(M)\mathcal{T}(M)$. The Talbot-Talbot inversion formula deals strictly with complex values. Due to the uneven spacing in nodes it may provide to be more accurate for less predictable or more variable functions. In this thesis, we will use the Talbot algorithm for the one-dimensional numerical Laplace inversion and the Talbot-Talbot algorithm for the two-dimensional numerical Laplace inversion.

Combination	Two-dimensional Function
$\mathcal{T}(M)\mathcal{G}(M)$:	$\frac{2 \ln(2)}{5t_1 t_2} \sum_{k_1=0}^{M-1} \operatorname{Re} \left\{ \gamma_{k_1} \sum_{k_2=1}^{2M} e_{k_2} \tilde{f} \left(\frac{\delta_{k_1}}{t_1}, \frac{k_2 \ln(2)}{t_2} \right) \right\}$
$\mathcal{T}(M)\mathcal{T}(M)$:	$\frac{2}{25t_1 t_2} \sum_{k_1=0}^{M-1} \operatorname{Re} \left\{ \gamma_{k_1} \sum_{k_2=0}^{M-1} \left[\gamma_{k_2} \tilde{f} \left(\frac{\delta_{k_1}}{t_1}, \frac{\delta_{k_2}}{t_2} \right) + \bar{\gamma}_{k_2} \tilde{f} \left(\frac{\delta_{k_1}}{t_1}, \frac{\bar{\delta}_{k_2}}{t_2} \right) \right] \right\}$
$\mathcal{E}(M)\mathcal{G}(M)$:	$\frac{10^{M/3} \ln(2)}{t_1 t_2} \sum_{k_1=0}^{2M} \eta_{k_1} \sum_{k_2=1}^{2M} e_{k_2} \operatorname{Re} \left\{ \tilde{f} \left(\frac{\beta_{k_1}}{t_1}, \frac{k_2 \ln(2)}{t_2} \right) \right\}$
$\mathcal{E}(M)\mathcal{T}(M)$:	$\frac{10^{M/3}}{5t_1 t_2} \sum_{k_1=0}^{2M} \eta_{k_1} \sum_{k_2=0}^{M-1} \operatorname{Re} \left\{ \gamma_{k_2} \tilde{f} \left(\frac{\beta_{k_1}}{t_1}, \frac{\delta_{k_2}}{t_2} \right) + \bar{\gamma}_{k_2} \tilde{f} \left(\frac{\beta_{k_1}}{t_1}, \frac{\bar{\delta}_{k_2}}{t_2} \right) \right\}$
$\mathcal{T}(M)\mathcal{E}(M)$:	$\frac{10^{M/3}}{5t_1 t_2} \sum_{k_1=0}^{M-1} \operatorname{Re} \left\{ \gamma_{k_1} \sum_{k_2=0}^{2M} \eta_{k_2} \left[\tilde{f} \left(\frac{\delta_{k_1}}{t_1}, \frac{\beta_{k_2}}{t_2} \right) + \tilde{f} \left(\frac{\delta_{k_1}}{t_1}, \frac{\bar{\beta}_{k_2}}{t_2} \right) \right] \right\}$
$\mathcal{G}(M)\mathcal{T}(3M)$:	$\frac{2 \ln(2)}{5t_1 t_2} \sum_{k_1=1}^{2M} e_{k_1} \sum_{k_2=1}^{3M-1} \operatorname{Re} \left\{ \gamma'_{k_2} \tilde{f} \left(\frac{k_1 \ln(2)}{t_1}, \frac{\delta'_{k_2}}{t_2} \right) \right\}$
$\mathcal{G}(M)\mathcal{G}(2M)$:	$\frac{(\ln(2))^2}{t_1 t_2} \sum_{k_1=1}^{2M} e_{k_1} \sum_{k_2=1}^{4M} e'_{k_2} \tilde{f} \left(\frac{k_1 \ln(2)}{t_1}, \frac{k_2 \ln(2)}{t_2} \right) \right\}$
$\mathcal{E}(M)\mathcal{E}(M)$:	$\frac{10^{2M/3}}{2t_1 t_2} \sum_{k_1=0}^{2M} \eta_{k_1} \sum_{k_2=0}^{2M} \eta_{k_2} \operatorname{Re} \left\{ \tilde{f} \left(\frac{\beta_{k_1}}{t_1}, \frac{\beta_{k_2}}{t_2} \right) + \tilde{f} \left(\frac{\beta_{k_1}}{t_1}, \frac{\bar{\beta}_{k_2}}{t_2} \right) \right\}$
$\mathcal{G}(M)\mathcal{E}(3M)$:	$\frac{10^M \ln(2)}{t_1 t_2} \sum_{k_1=1}^{2M} e_{k_1} \sum_{k_2=0}^{6M} \eta'_{k_2} \operatorname{Re} \left\{ \tilde{f} \left(\frac{k_1 \ln(2)}{t_1}, \frac{\beta'_{k_2}}{t_2} \right) \right\}$

Table 1.1: The nine two-dimensional Laplace inversion algorithms

1.5 Chapter Outline and Notations

The main objective of this thesis is to design and price some insurance products on stochastic drawdowns which provide investors the downside protection. These insurance products focus on the major risk measures of stochastic drawdowns, including the the severity of the drawdown event, frequency of drawdowns and speed of market crash. As the topic of insurance products using drawdowns is relatively new in this field, we believe it is of interest to view more possible products as a generalization, and build connections with the existing insurance/options in the market.

In Chapter 1, we introduce the concept of drawdowns and provide some preliminary results that are useful for the following chapters. To be more specific, we first discuss the related studies and the applications of how drawdowns are currently being used in different fields in Section 1.1. Then Section 1.2 provides the basic mathematical definitions for drawdown and drawdown-related quantities, such as the drawdown time, the maximum drawdown, and drawup. These quantities are used in later chapters to measure the risks when building our insurance/option's payoffs. We also provide a list of the options on drawdowns that have been studied in the past literature, which motivates the design of our proposed products. In Section 1.3, we discuss two risk models, namely the one-dimensional linear diffusion model and the spectrally negative Lévy process, and their scale functions and other properties. In Section 1.4, we introduce the main technique used in the thesis, the Laplace transform and its numerical

inversion. This is a key component to our pricing process.

In Chapter 2, we consider the fair market valuation of a drawdown insurance on the frequency and speed of market crash. We begin by introducing the frequency of drawdowns and speed of market crash in Section 2.1. The frequency of drawdowns is a series of drawdowns which can be defined under either with or without recovery scenario, and the speed of market crash captures the time spent on dropping from the running maximum to drawdown. Sections 2.3 and 2.4 are the model setup and the preliminary results for (geometric) Brownian motion. Then the proposed drawdown insurance and its valuation are done in Section 2.5 for drawdowns with and without recovery cases. We also discuss some variations that could be done in the contract design. Our pricing formulas are expressed in terms of the (two-dimensional) Laplace transforms, therefore we provide the numerical Laplace inversion results as well as sensitivity tests in Section 2.6.

In Chapter 3, we consider the fair market valuation of knock-in options on the size of drawdown risk, whose payoff depends on the size of the drawdown at maturity. Section 3.1 is the model setup, and similar to Chapter 2, we work on the drifted Brownian motion, as the log-surplus process. Preliminary results are then given in Section 3.2, where we view the drifted Brownian motion as a special case of spectrally negative Lévy process. In Section 3.3, we propose the knock-in drawdown options of interest with two types of payoffs, and find the expressions of the fair market prices in terms of Laplace transforms. Connections with the lookback put option and the digital option on maximum drawdown are discussed in Section 3.4. Lastly in Section 3.5, we compute the pricing using the numerical Laplace inversion and conduct the sensitivity tests. We also illustrate the consistency with the existing models numerically.

Finally, Chapter 4 concludes the thesis. We summarize our main results and contributions, and discuss some directions for future work that can be completed and how we can expand our current works into that.

Notations

Here we provide a breakdown of some important notation used in this thesis, as well as brief explanation to give clarity and consistency of variables, functions and more.

1_A - Indicator function for some event A

e_q - Exponential variable with mean $\frac{1}{q} > 0$

$\tau_X^\pm(x)$ - Exit times of process X reaching specified value x

$\tau_D^\pm(x)$ - Exit times of drawdown process D reaching specified value x (i.e., drawdown time and its recovery)

\bar{X} - Running maximum of process X .

\mathbb{E}_x - Expectation given $\{X_0 = x\}$. Note that we sometimes write $\mathbb{E}(\cdot) = \mathbb{E}_0(\cdot)$.

\mathbb{P}_x - Risk neutral probability measure given $\{X_0 = x\}$

$s(\cdot)$ - Scale function of linear diffusion process

$\Phi_q^\pm(\cdot)$ - Increasing/decreasing positive eigenfunction of linear diffusion process

$W_q(\cdot, \cdot), W_{q,1}(\cdot, \cdot)$ - Functions associated with linear diffusion process

$\psi(\cdot)$ - Laplace exponent of a spectrally negative Lévy process

$\Phi(q)$ - The largest solution to $\{\psi(x) = q\}$

$W_q(\cdot)$ - The q -scale function of a spectrally negative Lévy process

Chapter 2

Drawdown Insurance on the Frequency and Speed of Market Crash

In this chapter, we will design a drawdown insurance based on the frequency of drawdowns and the speed of market crash of each drawdown, and focus on its fair market price valuation. We will start with the introduction of the frequency of drawdowns and the speed of market crash.

2.1 Frequency of Drawdowns

Recall that, for a stochastic process $X = \{X_t\}_{t \geq 0}$, the (absolute) drawdown process is defined as

$$D_t = \bar{X}_t - X_t,$$

where $\bar{X}_t = \sup_{0 \leq s \leq t} X_s$ is its running maximum before time t , with $\bar{X}_0 = X_0$. Thus the drawdown size at time t is just the difference between the process's running maximum before time t and its current value.

The drawdown time (or more specific, absolute drawdown time) of size a is defined as

$$\tau_D^+(a) = \inf\{t \geq 0 : \bar{X}_t - X_t > a\}.$$

where a is a pre-fixed threshold for the (absolute) drawdown size. This could be viewed as the first drawdown time, denoted as $\tau_D^{1,+}(a) := \tau_D^+(a)$. Expanding this concept to a series of drawdown, one can consider the sequence of n drawdowns, for $n \geq 1$, which could be defined under two different scenarios: with and without recovery (see Chapter 4 of [18]):

- A drawdown **with recovery** means that after the previous drawdown occurs, the process X must reach back to its current running maximum \bar{X} before another drawdown can be considered; and
- A drawdown **without recovery** is simply restarting the process at the moment of a drawdown occurs with no need to return to the previous running maximum \bar{X} .

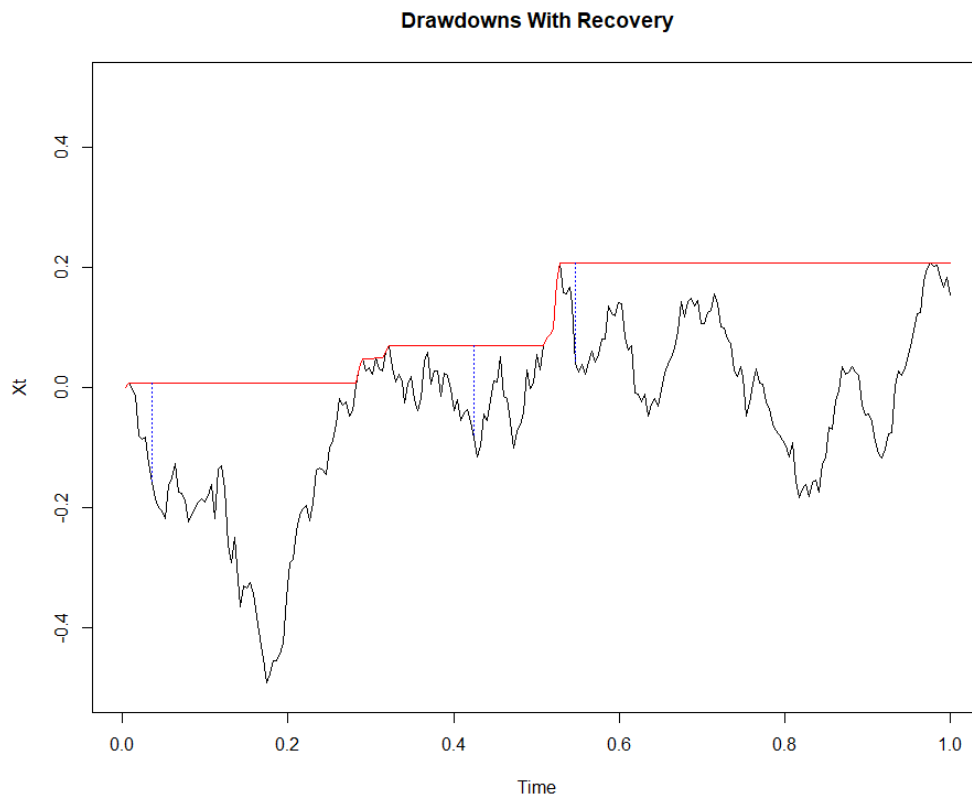


Figure 2.1: Illustration of multiple drawdowns with recovery.

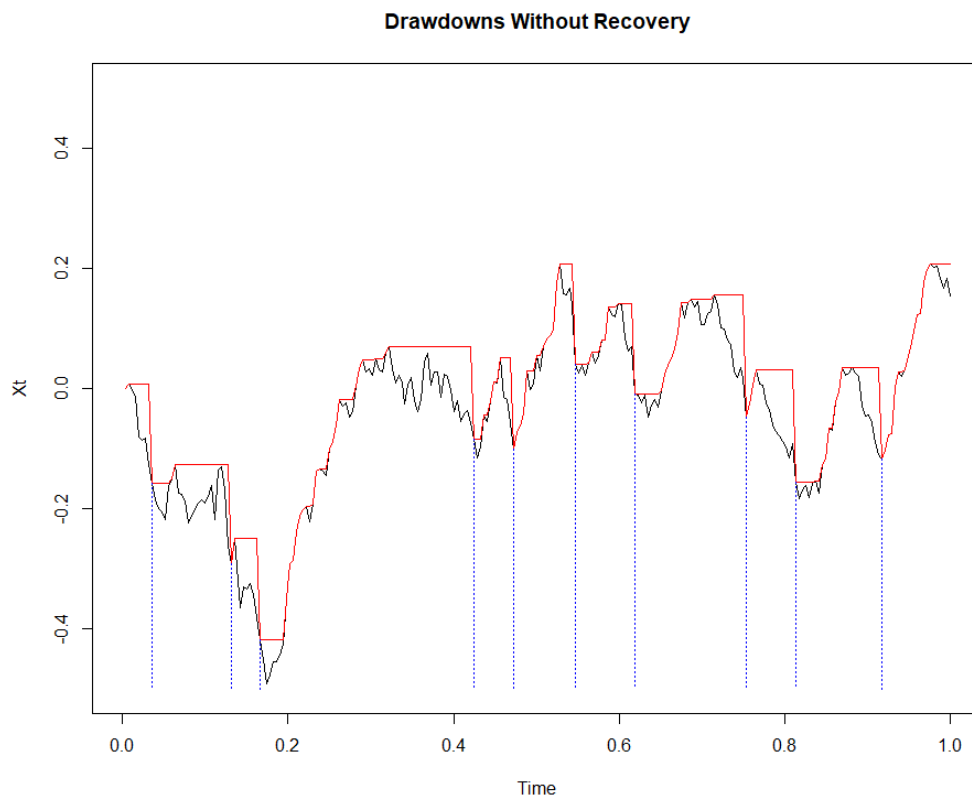


Figure 2.2: Illustration of multiple drawdowns without recovery.

Thus, for $n \geq 1$, the n^{th} drawdown times (of size a) with and without recovery, denoted by $\tilde{\tau}_D^{n,+}(a)$ and $\tau_D^{n,+}(a)$ respectively, are defined as

$$\tilde{\tau}_D^{n,+}(a) := \inf\{t > \tilde{\tau}_D^{n-1,+}(a) : \bar{X}_t - X_t > a, \bar{X}_t > \bar{X}_{\tilde{\tau}_D^{n-1,+}(a)}\}, \quad (2.1)$$

and

$$\tau_D^{n,+}(a) := \inf\{t > \tau_D^{n-1,+}(a) : \bar{X}_{[\tau_D^{n-1,+}(a), t]} - X_t > a\}, \quad (2.2)$$

where $\bar{X}_{[s,t]} = \sup_{s \leq u \leq t} X_u$ is the running maximum in the time interval $[s, t]$, and we use the convention that $\tilde{\tau}_D^{0,+}(a) = \tau_D^{0,+}(a) = 0$.

To visualize these two sequences of drawdown times, we illustrate the same sample path for with and without recovery cases in Figures 2.1 and 2.2 respectively. It can be seen from Figure 2.1 that the black line represents the sample path of our surplus process X_t , the red line represents the current maximum of the process \bar{X}_t until the time t , and lastly the dotted blue lines represent the exact drawdowns occurring with recovery. Figure 2.2 is similar, the difference being when there is no recovery required, the maximum process is reset to the current value at the time of the n^{th} drawdown, that is $X_{\tau_D^{n,+}(a)}$.

In addition, it can be easily shown that the series of the drawdown times with and without recovery have the following relationships. Their first drawdown times are the same, i.e.,

$$\tilde{\tau}_D^{1,+}(a) = \tau_D^{1,+}(a) = \tau_D^+(a), \quad a.s.,$$

as there is no need to recover the maximum when there is only one drawdown occurred. On the other hand, for the n^{th} drawdowns, due to the recovery requirements, $\tau_D^{n,+}(a) \leq \tilde{\tau}_D^{n,+}(a)$. Actually since larger drawdowns may occur during the recovering period, the drawdown times with recovery are in a subset of the drawdown times without recovery, i.e.,

$$\{\tilde{\tau}_D^{n,+}(a)\}_{n \geq 1} \subset \{\tau_D^{n,+}(a)\}_{n \geq 1}.$$

This can also be seen in Figures 2.1 and 2.2.

2.2 Speed of Market Crash

The speed of market crash is another measurement of drawdown risk recently introduced in [18]. In general, a drawdown event could be decomposed into the rising part and the crashing part. Figure 2.3 below illustrates this simply. As can be seen, the black line is the underlying process and the solid red line is the maximum of the process. It can be seen that the part from the start until the red line is considered the rising part, i.e., climbing up to the running maximum before a drawdown occurs. And the crashing part happens thereafter till the dotted blue line, i.e., dropping down to the drawdown of size a . The speed of market crash is then defined as the time spent in the crashing regime, in other words, the quantity of how quickly a drawdown occurs is used to describe the market crash. In practice, it is easier for the investor or fund manager to react to a slow market crash (from the maximum level) than a quick dramatic one.

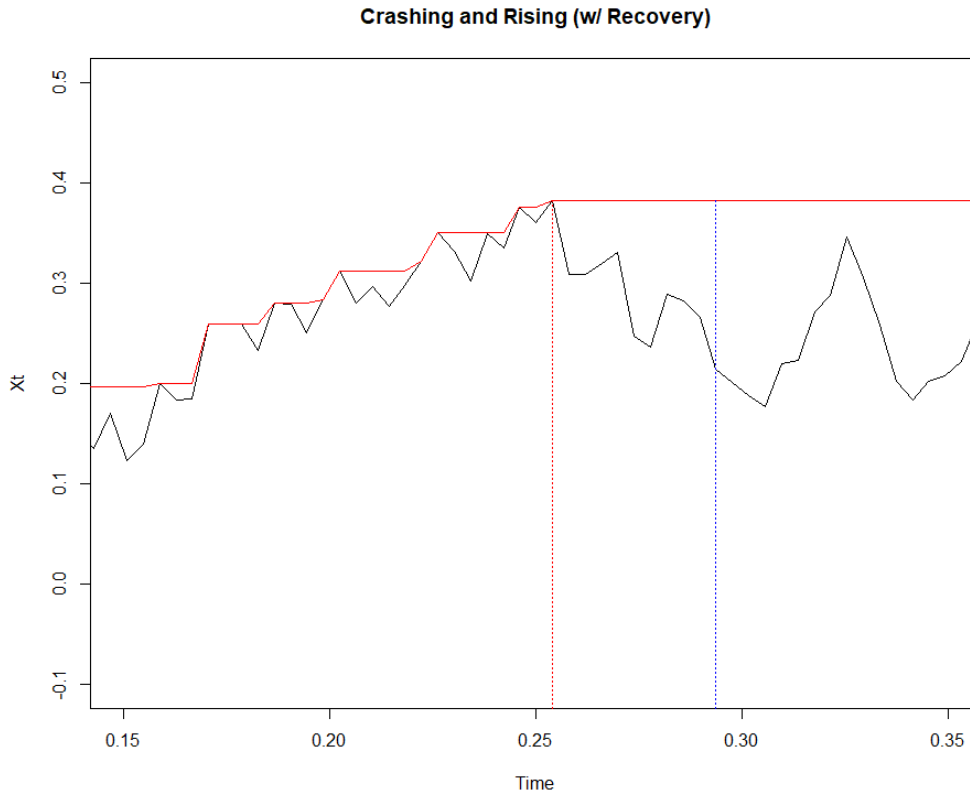


Figure 2.3: Rising and crashing part of drawdowns illustrated here.

To define the speed of market crash, we need to introduce another quantity related to the time of the last running maximum. Denote g_a as the last time of the running maximum before a drawdown of size a occurs,

$$g_a := \sup\{t < \tau_D^+(a) : X_t = \bar{X}_t\}, \quad (2.3)$$

and thus, the speed of the drawdown, denoted as S_a , is defined as

$$S_a := \tau_D^+(a) - g_a, \quad (2.4)$$

which is the time from the last maximum to when the drawdown of size a has occurred. This pair (g_a, S_a) can be viewed as the decomposition of the drawdown time. Now we will extend them further to the sequences of drawdowns. For $n \geq 1$, the last running maximum and the speed of a market crash for the n^{th} drawdown with recovery are defined as

$$\tilde{g}_a^n := \sup\{t < \tilde{\tau}_D^{n,+}(a) : X_t = \bar{X}_t\},$$

and

$$\tilde{S}_a^n := \tilde{\tau}_D^{n,+}(a) - \tilde{g}_a^n.$$

And similarly, the last running maximum and the speed of a market crash for the n^{th} drawdown without recovery are defined as

$$g_a^n := \sup\{\tau_D^{n-1,+}(a) < t < \tau_D^{n,+}(a) : X_t = \bar{X}_t\},$$

and

$$S_a^n := \tau_D^{n,+}(a) - g_a^n.$$

2.3 Model setup

In the following valuation of the proposed drawdown insurance, we assume the underlying asset $\mathbb{S} = \{\mathbb{S}_t\}_{t \geq 0}$ is modeled by a geometric Brownian motion, whose dynamics under the risk neutral measure \mathbb{Q} follows

$$d\mathbb{S}_t = r\mathbb{S}_t dt + \sigma\mathbb{S}_t dW_t, \quad \mathbb{S}_0 \in \mathbb{R}_+. \quad (2.5)$$

where $r \in \mathbb{R}_+$ is the risk free rate, $\sigma \in \mathbb{R}_+$ is the diffusion parameter, and $\{W_t\}_{t \geq 0}$ is a standard Brownian motion under measure \mathbb{Q} .

In practice, the proportional drawdowns, as relative to the underlying asset as a percentage, are often consider. For instance, a trailing stop order is widely used by investors to place a trailing stop loss when the value of the current position drops from its running maximum for more than a pre-specified percentage.

Denote the proportional drawdown of the underlying asset \mathbb{S} with a fixed percentage α by

$$T_{\mathbb{S}}^+(\alpha) := \inf\{t > 0 : \bar{\mathbb{S}}_t - \mathbb{S}_t > \alpha \bar{\mathbb{S}}_t\}, \quad (2.6)$$

for $0 < \alpha < 1$, where $\bar{\mathbb{S}}_t = \sup_{0 \leq s \leq t} \mathbb{S}_s$ is the maximum of our underlying process.

Under this model, it is well known that:

$$\mathbb{S}_t = \mathbb{S}_0 e^{X_t}. \quad (2.7)$$

where $X_t = (r - \frac{1}{2}\sigma^2)t + \sigma W_t$. In other words, the process $\{X_t\}$ with SDE

$$dX_t = \mu dt + \sigma dW_t, \quad (2.8)$$

follows Brownian motion (BM) with drift $\mu := r - \frac{1}{2}\sigma^2$ and diffusion coefficient $\sigma \in \mathbb{R}_+$. We can easily find a relationship between this proportional drawdown of $\{\mathbb{S}_t\}$ and the absolute drawdown of the corresponding drifted Brownian motion process $\{X_t\}$ by noticing that

$$\{\bar{\mathbb{S}}_t - \mathbb{S}_t > \alpha \bar{\mathbb{S}}_t\} = \{\bar{X}_t - X_t > -\log(1 - \alpha)\}.$$

Hence, by letting $a := -\log(1 - \alpha)$, we have

$$T_{\mathbb{S}}^+(\alpha) = \tau_D^+(a).$$

It is important to note that similar relationships could also be found for the frequency of drawdowns and the speed of market crash. Thanks to such relationships, in what follows, we only need to examine the quantities of interest related to the drifted BM $\{X_t\}$ as defined in the previous Sections 2.1 and 2.2.

In the following, all the expectations/probabilities are under measure \mathbb{Q} , hence we will omit it for simplicity.

2.4 Preliminary results of drifted BM

Consider the drifted BM process $X = \{X_t\}_{t \geq 0}$,

$$X_t = x + \mu t + \sigma W_t, \quad (2.9)$$

for $\mu, \sigma > 0$. For $q > 0$, let

$$\delta := \frac{\mu}{\sigma^2}, \quad \gamma_q := \sqrt{\delta^2 + \frac{2q}{\sigma^2}}.$$

Note that $\gamma_0 = \delta$. As a special case of the one-dimensional linear diffusion model, we have

$$s(x) = \begin{cases} \frac{1}{\delta}(1 - e^{-2\delta x}), & \mu \neq 0, \\ 2x, & \mu = 0. \end{cases}$$

Then the scale functions are given as

$$W_q(x, y) = 2e^{-\delta(x+y)} \frac{\sinh(\gamma_q(x-y))}{\gamma_q}, \quad (2.10)$$

and

$$W_{q,1}(x, y) = \gamma_q \coth(\gamma_q(x-y)) - \delta.$$

Recall the following result of Theorem 3.1 of [18] (pg. 44) under the linear diffusion model is given as follows.

Lemma 2.4.1 *For $q, p, \rho > 0$ and X being the one-dimensional linear diffusion model, the joint LT of the triplet (g_a, S_a, X_{g_a}) is given as*

$$\mathbb{E}_x(e^{-qg_a - \rho S_a - \rho X_{g_a}}) = \int_x^r \frac{e^{-\rho m} s'(m)}{W_p(m, m-a)} \exp\left(-\int_x^m W_{q,1}(u, u-a) du\right) dm, \quad \forall x \in I. \quad (2.11)$$

where the scale function $s(\cdot)$ and functions $W_q(\cdot, \cdot)$, $W_{q,1}(\cdot, \cdot)$ are defined as in Section 1.3.1.

A simplification under the drifted BM model gives the following lemma.

Lemma 2.4.2 *For $q, p, \rho > 0$ and the process X follows drifted BM as in (2.9), we have*

$$\mathbb{E}_0(e^{-qg_a - \rho S_a - \rho X_{g_a}}) = \frac{\gamma_p e^{-\delta a}}{\sinh(\gamma_p a) \rho + \gamma_q \coth(\gamma_q a) - \delta}. \quad (2.12)$$

and a direct LT inversion with respect to ρ , gives, for $y > 0$,

$$\mathbb{E}_0(e^{-qg_a - \rho S_a} 1_{\{X_{g_a} \in dy\}}) = \frac{\gamma_p e^{-\delta a}}{\sinh(\gamma_p a)} e^{-(\gamma_q \coth(\gamma_q a) - \delta)y} dy. \quad (2.13)$$

Proof We begin by using the result of (2.11) from Chapter 1 and setting $X_0 = x = 0$, $r = \infty$. We can first find the results of the scale functions based on the formulas previously listed under drifted BM as such

$$s'(m) = 2e^{-2\delta m}$$

by taking the derivative of the scale function $s(x)$ and setting $x = m$. We can do the same to find $W_p(m, m - a)$ and $W_{q,1}(u, u - a)$ as the following

$$W_p(m, m - a) = 2e^{-\delta(2m-a)} \frac{\sinh(\gamma_p a)}{\gamma_p},$$

$$W_{q,1}(u, u - a) = \gamma_q \coth(\gamma_q a) - \delta.$$

With all the formulas set under drifted BM, now simply substitute these back into (2.11) and integrate w.r.t both u and m respectively as such

$$\begin{aligned} \mathbb{E}_0(e^{-qg_a - pS_a - \rho X_{g_a}}) &= \int_0^\infty \frac{e^{-\rho m} 2e^{-2\delta m}}{2e^{-2\delta m} e^{\delta a} \frac{\sinh(\gamma_p a)}{\gamma_p}} e^{-\int_0^m (\gamma_q \coth(\gamma_q a) - \delta) du} dm \\ &= \int_0^\infty \frac{e^{-\rho m} e^{-\delta a} \gamma_p}{\sinh(\gamma_p a)} e^{-m(\gamma_q \coth(\gamma_q a) - \delta)} dm \\ &= \frac{\gamma_p e^{-\delta a}}{\sinh(\gamma_p a)} \int_0^\infty e^{-\rho m} e^{-m(\gamma_q \coth(\gamma_q a) - \delta)} dm \\ &= \frac{\gamma_p e^{-\delta a}}{\sinh(\gamma_p a)} \int_0^\infty e^{-m(\rho + \gamma_q \coth(\gamma_q a) - \delta)} dm \\ &= \frac{\gamma_p e^{-\delta a}}{\sinh(\gamma_p a)} \frac{1}{\rho + \gamma_q \coth(\gamma_q a) - \delta} \end{aligned}$$

which is the result given in (2.12). Simply taking the Laplace inversion w.r.t ρ gives the result in (2.13) and this completes the proof.

This lemma is important for the calculation in the subsequent sections. Further, we let

$$G(q, p, \rho) := \mathbb{E}_0(e^{-qg_a - pS_a - \rho X_{g_a}}), \quad (2.14)$$

and in the drifted BM case from the above lemma, by letting $\rho = 0$, we have

$$G(q, p) := G(q, p, 0) = \mathbb{E}_0(e^{-qg_a - pS_a}) = \frac{\gamma_p e^{-\delta a}}{\sinh(\gamma_p a)} \frac{1}{\gamma_q \coth(\gamma_q a) - \delta}. \quad (2.15)$$

Lemma 2.4.3 *For $q > 0$ and the process X follows drifted BM as in (2.9), the LT of the (one-sided) exit time from above is given*

$$\mathbb{E}_0(e^{-q\tau_X^+(z)}) = e^{-(\gamma_q - \delta)z}.$$

Proof Considering drifted BM as a special case of a linear diffusion model, we will start with the well known two-sided exit result of a linear diffusion model from [18] that

$$\mathbb{E}_x(e^{-q\tau_X^+(z)} \mathbf{1}_{\{\tau_X^+(z) < \tau_X^-(y)\}}) = \frac{W_q(y, x)}{W_q(y, z)}.$$

Using the previously defined $W_q(x, y)$ function in Equation (2.10) and letting $y \rightarrow \infty$, we have

$$\begin{aligned}
\lim_{y \rightarrow -\infty} \frac{W_q(y, x)}{W_q(y, z)} &= \lim_{y \rightarrow -\infty} \frac{e^{-\delta(y+x)} \cdot \sinh(\gamma_q(y-x))}{e^{-\delta(y+z)} \cdot \sinh(\gamma_q(y-z))} \\
&= e^{\delta(z-x)} \lim_{y \rightarrow -\infty} \frac{\sinh(\gamma_q(y-x))}{\sinh(\gamma_q(y-z))} \\
&= e^{\delta(z-x)} \lim_{y \rightarrow -\infty} \frac{-e^{-\gamma_q(-x+y)} + e^{\gamma_q(-x+y)}}{-e^{-\gamma_q(-z+y)} + e^{\gamma_q(-z+y)}} \\
&= e^{\delta(z-x)} \lim_{y \rightarrow -\infty} e^{\gamma_q(z-x)} \frac{-e^{2\gamma_q x} + e^{2\gamma_q y}}{-e^{2\gamma_q z} + e^{2\gamma_q y}} \\
&= e^{\delta(z-x)} e^{\gamma_q(z-x)} \frac{\lim_{y \rightarrow -\infty} (-e^{2\gamma_q x} + e^{2\gamma_q y})}{\lim_{y \rightarrow -\infty} (-e^{2\gamma_q z} + e^{2\gamma_q y})} \\
&= e^{\delta(z-x)} e^{\gamma_q(z-x)} \left(\frac{-e^{2\gamma_q x}}{-e^{2\gamma_q z}} \right) \\
&= e^{-(\gamma_q - \delta)(z-x)}.
\end{aligned}$$

By setting $X_0 = x = 0$, we obtain the result given in the lemma and complete the proof.

2.5 The valuation of a drawdown insurance

In this section, we propose a drawdown insurance contract whose claim size depends on the number of market crashes before maturity. This can be used as protection against the risks of market crashes. A pre-specified threshold (or strike) level $b > 0$ is considered to measure the seriousness of market crashes, in other words, if the speed of market crash is less than b , we consider it as one market crash event. Thus, our proposed insurance contract has claim size of $\$k$ dollars at maturity time T , given that k market crashes occur before maturity. We will discuss two types of this contract depending on whether the sequence of drawdowns is considered with or without recovery, and within each case, we consider other variations of the claim payment. We believe these contracts provide the policyholder more options, so that they could choose the one of their best interest. We begin with the case of drawdown times without recovery.

2.5.1 Without recovery case

Contract I: Consider that the insurance product pays $\$k$ dollars at maturity time T , given that k market crashes occur before maturity.

In this subsection, we consider the sequence of drawdown times are of without recovery case.

Let $N_T^X(a, b)$ be the number of drawdowns of size a with speed of market crash $S_a^k < b$. Then we can write out $N_T^X(a, b)$ mathematically,

$$N_T^X(a, b) = \sum_{n=1}^{\infty} \mathbf{1}_{\{\tau_D^{n,+}(a) \leq T, S_a^n < b\}}. \quad (2.16)$$

Note that if no drawdown occurs before maturity, the payment amount is 0.

By the design of the insurance contract, its risk-neutral price is given by

$$V(T, b) := e^{-rT} \mathbb{E}(N_T^X(a, b)) = e^{-rT} \sum_{n=1}^{\infty} \mathbb{E}(1_{\{\tau_D^{n,+}(a) \leq T, S_a^n < b\}}). \quad (2.17)$$

We will solve this by taking the Laplace transform (LT) with respect to T and b , and then numerically take the Laplace inversion for the valuation purpose. This is essentially same as the technique of randomizing the maturity time T and threshold level b by letting $T = e_q$ and $b = e_s$, where e_q and e_s are two independent exponential random variables with means $1/q$ and $1/s$ respectively.

Proposition 2.5.1 (Without recovery case.) *For $q, s > 0$ and r being the risk-free rate, we have the LT of the fair market value defined in Equation (2.17) as*

$$\int_0^{\infty} \int_0^{\infty} e^{-qT} e^{-sb} V(T, b) dT db = \frac{1}{(q+r)s} \frac{G(q+r, q+r+s)}{1-G(q+r, q+r)},$$

where

$$G(q, p) = \frac{\gamma_p e^{-\delta a}}{\sinh(\gamma_p a)} \frac{1}{\gamma_q \coth(\gamma_q a) - \delta}.$$

Proof First we can simplify the double integration of LT by plugging in the price formula

$$\begin{aligned} \int_0^{\infty} \int_0^{\infty} e^{-qT} e^{-sb} V(T, b) dT db &= \int_0^{\infty} \int_0^{\infty} e^{-(q+r)T} e^{-sb} \mathbb{E}(N_T^X(a, b)) dT db \\ &= \frac{1}{q+r} \cdot \frac{1}{s} \int_0^{\infty} \int_0^{\infty} (q+r) e^{-(q+r)T} s e^{-sb} \sum_{n=1}^{\infty} \mathbb{E}(1_{\{\tau_D^{n,+}(a) \leq T, S_a^n < b\}}) dT db \\ &= \frac{1}{q+r} \cdot \frac{1}{s} \sum_{n=1}^{\infty} \mathbb{E}(1_{\{\tau_D^{n,+}(a) < e_{q+r}, S_a^n < e_s\}}) \\ &= \frac{1}{(q+r)s} \sum_{n=1}^{\infty} \mathbb{E}(e^{-(q+r)\tau_D^{n,+}(a) - sS_a^n}), \end{aligned} \quad (2.18)$$

where the last step use the tail distribution of the (independent) exponential random variables e_{q+r} and e_s .

Then we realize the fact that when dealing with drawdown times without recovery, due to the strong Markov property of the BM, the renewal argument applies after each drawdown time. Also, note that the drawdown times as well as the speed of market crash are independent of the initial surplus level. Hence, by conditioning on the first drawdown, we get the following result as renewal happens at the drawdown time, for any $n > 1$,

$$\begin{aligned} \mathbb{E}(e^{-(q+r)\tau_D^{n,+}(a) - sS_a^n}) &= \mathbb{E}(e^{-(q+r)\tau_D^+(a)}) \mathbb{E}(e^{-(q+r)\tau_D^{n-1,+}(a) - sS_a^{n-1}}) \\ &= \mathbb{E}(e^{-(q+r)\tau_D^+(a) - sS_a}) [\mathbb{E}(e^{-(q+r)\tau_D^+(a)})]^{n-1} \\ &= \mathbb{E}(e^{-(q+r)g_a - (q+r+s)S_a}) [\mathbb{E}(e^{-(q+r)g_a - (q+r)S_a})]^{n-1} \\ &= G(q+r, q+r+s) \times G(q+r, q+r)^{n-1} \end{aligned} \quad (2.19)$$

where the $G(\cdot, \cdot)$ function is the joint LT of g_a and S_a , which is given in Equation (2.15). And the third line is due to the relationship $\tau_D^+(a) = g_a + S_a$. Note that Equation (2.19) also holds for the case of $n = 1$. Substituting (2.19) back into (2.18) completes the proof.

Here we make two remarks about our results.

Remark 1 (Connections to existing results). Note that when $b \geq T$, $\{\tau_D^{n,+}(a) \leq T, S_a^n < b\} = \{\tau_D^{n,+}(a) \leq T\}$, hence we drop the argument on the speed of market crash,

$$V(T, b)|_{\{b \geq T\}} = e^{-rT} \sum_{n=1}^{\infty} \mathbb{E}(1_{\{\tau_D^{n,+}(a) \leq T\}}),$$

which was the insurance of frequent relative drawdowns discussed in [12]. In this case, all the argument with respect to variable s could be dropped, and our results are consistent with [12]. And this consistency are also seen in the numerical calculation in the next section.

Remark 2 (Other variations). Note that such insurance contract could also have other variations, which can be similarly analyzed. We discuss the following two variations as examples.

- (i) One possible variation is the type that the insurer pays the policyholder \$1 at the time of each market crash event as long as it happens before maturity, which has the risk-neutral price

$$V_{\tau}(T, b) := \sum_{n=1}^{\infty} \mathbb{E}(e^{-r\tau_D^{n,+}(a)} 1_{\{\tau_D^{n,+}(a) \leq T, S_a^n < b\}}). \quad (2.20)$$

Following similar methodology as above, we will show the result of this type of insurance in Proposition 2.5.2.

- (ii) Another possible variation is to add a knock-out barrier B for each market crash payment, i.e., if the surplus level reaches this barrier during a specific drawdown event, the \$1 payment will not be made. The risk-neutral price of this policy is

$$V_B(T, b) := e^{-rT} \sum_{n=1}^{\infty} \mathbb{E}_x(1_{\{\tau_D^{n,+}(a) \leq T, S_a^n < b, X_{s_a^n} < B\}}). \quad (2.21)$$

Note that the valuation of $V_B(T, b)$ depends on the initial surplus level x now. As B goes to ∞ , this policy should converge to the original contract, i.e.,

$$\lim_{B \rightarrow \infty} V_B(T, b) = V(T, b).$$

We present its fair market valuation (in terms of Laplace transform) in Proposition 2.5.3.

Proposition 2.5.2 For $q, s > 0$, the LT of the fair market value $V_{\tau}(T, b)$ defined in Equation (2.20) is given as

$$\int_0^{\infty} \int_0^{\infty} e^{-qT} e^{-sb} V_{\tau}(T, b) dT db = \frac{1}{q \cdot s} \frac{G(q+r, q+r+s)}{1 - G(q+r, q+r)},$$

where r is the risk-free rate and $G(q, p) = \frac{\gamma_p e^{-\delta a}}{\sinh(\gamma_p a)} \frac{1}{\gamma_q \coth(\gamma_q a) - \delta}$.

Proof Considering the double integration of LT by plugging in the price formula, we have

$$\begin{aligned}
\int_0^\infty \int_0^\infty e^{-qT} e^{-sb} V_\tau(T, b) dT db &= \int_0^\infty \int_0^\infty e^{-qT} e^{-sb} \sum_{n=1}^\infty \mathbb{E}(e^{-r\tau_D^{n,+}(a)} 1_{\{\tau_D^{n,+}(a) \leq T, S_a^n < b\}}) dT db \\
&= \frac{1}{qs} \int_0^\infty \int_0^\infty qe^{-qT} se^{-sb} \sum_{n=1}^\infty \mathbb{E}(e^{-r\tau_D^{n,+}(a)} 1_{\{\tau_D^{n,+}(a) \leq T, S_a^n < b\}}) dT db \\
&= \frac{1}{qs} \sum_{n=1}^\infty \mathbb{E}(e^{-r\tau_D^{n,+}(a)} 1_{\{\tau_D^{n,+}(a) < e_q, S_a^n < e_s\}}) \\
&= \frac{1}{qs} \sum_{n=1}^\infty \mathbb{E}(e^{-(q+r)\tau_D^{n,+}(a) - sS_a^n}),
\end{aligned}$$

where the last step use the tail distribution of the (independent) exponential random variables e_q and e_s . And the rest of the proof is same as in Proposition 2.4.1.

Proposition 2.5.3 For $q, s > 0$, the LT of the fair market value of the policy with the knock-out barrier defined in Equation (2.21) is given as

$$\begin{aligned}
&\int_0^\infty \int_0^\infty e^{-qT} e^{-sb} V_B(T, b) dT db \\
&= \frac{1}{(q+r)s} \frac{\gamma_{q+r+s} e^{-\delta a}}{\lambda_{q+r} \sinh(\gamma_{q+r+s} a)} \sum_{n=1}^\infty \left(\frac{\gamma_{q+r} e^{-\delta a}}{\lambda_{q+r} \sinh(\gamma_{q+r} a)} \right)^{n-1} \left(1 - \sum_{m=0}^{n-1} \frac{(\lambda_{q+r}(B-x+(n-1)a))^m}{m!} e^{-\lambda_{q+r}(B-x+(n-1)a)} \right),
\end{aligned}$$

where r is the risk-free rate and $\lambda_{q+r} = \gamma_{q+r} \coth(\gamma_{q+r} a) - \delta$.

Proof Following the similar methodology in the previous proposition, we can show that

$$\int_0^\infty \int_0^\infty e^{-qT} e^{-sb} V_B(T, b) dT db = \frac{1}{(q+r)s} \sum_{n=1}^\infty \mathbb{E}_x(e^{-(q+r)\tau_D^{n,+}(a) - sS_a^n} 1_{\{X_{g_a^n} < B\}}). \quad (2.22)$$

To find $\mathbb{E}_x(e^{-(q+r)\tau_D^{n,+}(a) - sS_a^n} 1_{\{X_{g_a^n} < B\}})$ in the above equation, we use another LT argument.

Considering the joint LT of $(\tau_D^{n,+}(a), S_a^n, X_{g_a^n} + (n-1)a)$, by the strong Markov property of the underlying process, one has

$$\begin{aligned}
\mathbb{E}_0(e^{-(q+r)\tau_D^{n,+}(a) - sS_a^n - \beta(X_{g_a^n} + (n-1)a)}) &= \mathbb{E}_0(e^{-(q+r)\tau_D^{n,+}(a) - sS_a^n - \beta(X_{\tau_D^{n,+}(a)} + na)}) \\
&= \mathbb{E}_0(e^{-(q+r)\tau_D^+(a) - \beta(X_{\tau_D^+(a)} + a)}) \mathbb{E}_0(e^{-(q+r)\tau_D^{n-1,+}(a) - sS_a^{n-1} - \beta(X_{\tau_D^{n-1,+}(a)} + (n-1)a)}),
\end{aligned}$$

and recursively, it becomes

$$\begin{aligned}
\mathbb{E}_0(e^{-(q+r)\tau_D^{n,+}(a) - sS_a^n - \beta(X_{g_a^n} + (n-1)a)}) &= [\mathbb{E}_0(e^{-(q+r)\tau_D^+(a) - \beta(X_{\tau_D^+(a)} + a)})]^{n-1} \mathbb{E}_0(e^{-(q+r)\tau_D^+(a) - sS_a - \beta(X_{\tau_D^+(a)} + a)}) \\
&= [\mathbb{E}_0(e^{-(q+r)g_a - (q+r)S_a - \beta(X_{\tau_D^+(a)} + a)})]^{n-1} \mathbb{E}_0(e^{-(q+r)g_a - (q+r+s)S_a - \beta(X_{\tau_D^+(a)} + a)}) \\
&= [G(q+r, q+r, \beta)]^{n-1} G(q+r, q+r+s, \beta) \\
&= \left(\frac{\gamma_{q+r} e^{-\delta a}}{\sinh(\gamma_{q+r} a)} \right)^{n-1} \frac{\gamma_{(q+r)+s} e^{-\delta a}}{\sinh(\gamma_{(q+r)+s} a)} \left(\frac{1}{\beta + \gamma_{q+r} \coth(\gamma_{q+r} a) - \delta} \right)^n.
\end{aligned}$$

where the last line plugs in the expression of $G(q, p, \rho)$ in Lemma 2.4.2.

Hence, the LT inversion with respect to the argument β yields the Erlang density (without the term $(\lambda_{q+r})^n$),

$$\mathbb{E}_0(e^{-(q+r)\tau_D^{n+}(a)-sS_a^n} \mathbf{1}_{\{X_{s_a^n}^{n+}(n-1)a \in dy\}}) = \left(\frac{\gamma_{q+r} e^{-\delta a}}{\sinh(\gamma_{q+r} a)} \right)^{n-1} \frac{\gamma_{(q+r)+s} e^{-\delta a}}{\sinh(\gamma_{(q+r)+s} a)} \frac{y^{n-1} e^{-\lambda_{q+r} y}}{(n-1)!} dy, \quad y > 0,$$

where let $\lambda_{q+r} := \gamma_{q+r} \coth(\gamma_{q+r} a) - \delta$. Therefore, using the shift argument and an integration over y gives

$$\begin{aligned} & \mathbb{E}_x(e^{-(q+r)\tau_D^{n+}(a)-sS_a^n} \mathbf{1}_{\{X_{s_a^n}^{n+} < B\}}) \\ &= \mathbb{E}_0(e^{-(q+r)\tau_D^{n+}(a)-sS_a^n} \mathbf{1}_{\{X_{s_a^n}^{n+} < B-x\}}) \\ &= \mathbb{E}_0(e^{-(q+r)\tau_D^{n+}(a)-sS_a^n} \mathbf{1}_{\{X_{s_a^n}^{n+}(n-1)a < B-x+(n-1)a\}}) \\ &= \int_0^{B-x+(n-1)a} \left(\frac{\gamma_{q+r} e^{-\delta a}}{\sinh(\gamma_{q+r} a)} \right)^{n-1} \frac{\gamma_{(q+r)+s} e^{-\delta a}}{\sinh(\gamma_{(q+r)+s} a)} \frac{y^{n-1} e^{-\lambda_{q+r} y}}{(n-1)!} dy \\ &= \left(\frac{\gamma_{q+r} e^{-\delta a}}{\sinh(\gamma_{q+r} a)} \right)^{n-1} \frac{\gamma_{(q+r)+s} e^{-\delta a}}{\sinh(\gamma_{(q+r)+s} a)} \int_0^{B-x+(n-1)a} \frac{y^{n-1} e^{-\lambda_{q+r} y}}{(n-1)!} dy \\ &= \left(\frac{\gamma_{q+r} e^{-\delta a}}{\sinh(\gamma_{q+r} a)} \right)^{n-1} \frac{\gamma_{q+r+s} e^{-\delta a}}{\sinh(\gamma_{q+r+s} a)} \frac{1}{(\lambda_{q+r})^n} \left(1 - \sum_{m=0}^{n-1} \frac{(\lambda_{q+r}(B-x+(n-1)a))^m}{m!} e^{-\lambda_{q+r}(B-x+(n-1)a)} \right), \end{aligned}$$

where in the second last step, the remaining components are multiplied and divided by $(\lambda_{q+r})^n$, and we are simply left with an Erlang density function. As such, we are able to integrate this and get the cumulative distribution function (cdf) of the Erlang distribution (see the remark below). Finally, substituting back to (2.22) we complete the proof.

Remark The Erlang distribution, denoted $Erlang(k, \lambda)$, has the probability density function

$$f(x) = \frac{\lambda^k x^{k-1} e^{-\lambda x}}{(k-1)!}, \quad x > 0,$$

where the parameters $k \in \mathbb{N}_+$ and $\lambda \in \mathbb{R}_+$ are called the shape and rate parameters respectively. It is essentially a Gamma distribution with integer shape parameters, and in the case of $k = 1$, it reduces to the exponential distribution with mean $1/\lambda$. The cumulative distribution function of $Erlang(k, \lambda)$ is

$$F(x) = 1 - \sum_{n=0}^{k-1} \frac{1}{n!} e^{-\lambda x} (\lambda x)^n,$$

and its LT transform is

$$\tilde{f}(s) = \left(\frac{\lambda}{\lambda + s} \right)^k.$$

2.5.2 With recovery case

In this subsection, we consider the Contract I with recovery case. More specifically, the insurance product pays \$k\$ dollars at maturity time T , given that k market crashes occur before maturity, and the sequence of drawdown times are considered with recovery. Each of the k market crashes has to occur after the previous drawdown's running maximum is recovered. As before, the tilde notation $\tilde{\cdot}$ is used to indicate the recovery case. That is, we let $\tilde{N}_T^X(a, b)$ be the number of drawdowns of size a with speed of market crash $\tilde{S}_a^k < b$. Then we can give this expression as:

$$\tilde{N}_T^X(a, b) = \sum_{n=1}^{\infty} \mathbf{1}_{\{\tilde{\tau}_D^{n,+}(a) \leq T, \tilde{S}_a^n < b\}}. \quad (2.23)$$

In this case, the fair market price can be defined as

$$\tilde{V}(T, b) := e^{-rT} \mathbb{E}(\tilde{N}_T^X(a, b)) = e^{-rT} \sum_{n=1}^{\infty} \mathbb{E}(\mathbf{1}_{\{\tilde{\tau}_D^{n,+}(a) \leq T, \tilde{S}_a^n < b\}}). \quad (2.24)$$

It can be seen here that the solution for the drawdown insurance with recovery is very similar to the previous Section 2.5.1 on drawdown insurances without recovery. The difference is when we apply the renewal argument, we need to consider the reaching back of previous running maximum of the process X . Based on this idea, we have the following result.

Proposition 2.5.4 (With recovery case.) *For $q, s > 0$, we have the LT of the fair market value*

$$\int_0^{\infty} \int_0^{\infty} e^{-qT} e^{-sb} \tilde{V}(T, b) dT db = \frac{1}{(q+r)s} \frac{G(q+r, q+r+s)}{1 - e^{-(\gamma_{q+r}-\delta)a} G(q+r, q+r)}.$$

Proof We start by simplifying the double integration of the LT using the randomizing technique as we did previously,

$$\begin{aligned} \int_0^{\infty} \int_0^{\infty} e^{-qT} e^{-sb} \tilde{V}(T, b) dT db &= \int_0^{\infty} \int_0^{\infty} e^{-(q+r)T} e^{-sb} \mathbb{E}(\tilde{N}_T^X(a, b)) dT db \\ &= \frac{1}{(q+r)s} \sum_{n=1}^{\infty} \mathbb{E}(e^{-(q+r)\tilde{\tau}_D^{n,+}(a)-s\tilde{S}_a^n}) \end{aligned} \quad (2.25)$$

Then due to the Markov property, the inter-drawdown times are independent from each other, so we can apply the renewal argument. Similarly as before, we can recursively determine the expectation by conditioning on the first drawdown time $\tau_D^+(a)$ and the recovery time $\tau_X^+(a)$ (since the drawdown size is a), and get the following result as

$$\begin{aligned} \mathbb{E}(e^{-(q+r)\tilde{\tau}_D^{n,+}(a)-s\tilde{S}_a^n}) &= \mathbb{E}(e^{-(q+r)\tau_D^+(a)}) \mathbb{E}(e^{-(q+r)\tau_X^+(a)}) \mathbb{E}(e^{-(q+r)\tilde{\tau}_D^{n-1,+}(a)-s\tilde{S}_a^{n-1}}) \\ &= [\mathbb{E}(e^{-(q+r)\tau_D^+(a)}) \mathbb{E}(e^{-(q+r)\tau_X^+(a)})]^{n-1} \mathbb{E}(e^{-(q+r)\tau_D^+(a)-sS_a}) \\ &= [\mathbb{E}(e^{-(q+r)g_a-(q+r)S_a}) \mathbb{E}(e^{-(q+r)\tau_X^+(a)})]^{n-1} \mathbb{E}(e^{-(q+r)g_a-(q+r+s)S_a}) \\ &= \left(G(q+r, q+r) e^{-(\gamma_{q+r}-\delta)a} \right)^{n-1} G(q+r, q+r+s) \end{aligned} \quad (2.26)$$

which holds for any $n \geq 1$. Lemmas 2.4.2 and 2.4.3 are used here.

Substituting (2.26) back into (2.25), which becomes the sum of an infinite geometric series, completes the proof.

Note that the variations of our drawdown insurance contract that are discussed in the previous section, can be also similarly analyzed.

2.6 Numerical results on two-dimensional LT Inversion

The valuation formulas in the previous section are given in the form of two-dimensional Laplace transform. For instance, in Propositions 2.4.1 and 2.4.4., the LTs of the fair market value of Contract I without and with recovery case are given as, respectively,

$$\tilde{f}_1(q, s) = \int_0^\infty \int_0^\infty e^{-sb-qT} V(T, b) dT db = \frac{1}{(q+r)s} \frac{G(q+r, q+r+s)}{1-G(q+r, q+r)},$$

and

$$\tilde{f}_2(q, s) = \int_0^\infty \int_0^\infty e^{-sb-qT} \tilde{V}(T, b) dT db = \frac{1}{(q+r)s} \frac{G(q+r, q+r+s)}{1-e^{-(\gamma_{q+r}-\delta)a} G(q+r, q+r)}.$$

The direct inversions with respect to both arguments q and s can not be done easily, hence we will rely on the methods for numerically inverting a two-dimensional LT. The three main algorithms, namely, Gaver-Stehfest, Euler and Talbot algorithms, for one-dimensional Laplace inversion, and their combination yields nine possible ways for a two-dimensional Laplace transform inversion. In this section, we particularly use the Talbot-Talbot algorithm $\mathcal{T}(M)\mathcal{T}(M)$ defined as (see Section 1.5.3 for more details):

$$f(t_1, t_2) = \frac{2}{25t_1t_2} \sum_{k_1=0}^{M-1} \operatorname{Re} \left\{ \gamma_{k_1} \sum_{k_2=0}^{M-1} \left[\gamma_{k_2} \tilde{f}\left(\frac{\delta_{k_1}}{t_1}, \frac{\delta_{k_2}}{t_2}\right) + \bar{\gamma}_{k_2} \tilde{f}\left(\frac{\delta_{k_1}}{t_1}, \frac{\bar{\delta}_{k_2}}{t_2}\right) \right] \right\}, \quad (2.27)$$

where M is the precision parameter for Laplace inversion.

This process was completed in R based on specified values for the drawdown size a , risk free rate r , and volatility σ . The parameters used in our numerical example are

- risk-free rate $r = 0.05$;
- proportional drawdown parameter $\alpha = 0.15$, or equivalently the (absolute) drawdown size is $a = -\log(1 - \alpha)$;
- volatility $\sigma = 0.10$.

And the parameter M is chosen to be 50.

Tables 2.1 and 2.2 are the resulting Laplace transform inversion for the drawdown insurance Contract I without and with recovery cases, respectively. They show the contract value $V(T, b)$ and $\tilde{V}(T, b)$ as a function of different maturity times T and thresholds b .

From Tables 2.1 and 2.2, we see that the results given for both without and with recovery are as expected.

As the threshold b increases, the fair market value increases, as there will be more market crashes counted in the claims for a fixed maturity time T . For the case of $b < T$, the speed of market crash is not guaranteed, so the price ends up being lower as if the drawdown does not

b	0.5	1	1.5	2	2.5	3
$T = 0.5$	0.0217	0.0218	0.0218	0.0218	0.0218	0.0218
$T = 1$	0.0569	0.1102	0.1102	0.1102	0.1102	0.1102
$T = 1.5$	0.0837	0.1857	0.2075	0.2075	0.2075	0.2075
$T = 2$	0.1088	0.2518	0.2931	0.3010	0.3011	0.3011
$T = 2.5$	0.1326	0.3143	0.3719	0.3871	0.3900	0.3900
$T = 3.5$	0.1552	0.3734	0.4466	0.4678	0.4732	0.4743

Table 2.1: Numerical results for $V(T, b)$ Contract I without recovery case

b	0.5	1	1.5	2	2.5	3
$T = 0.5$	0.0217	0.0218	0.0218	0.0218	0.0218	0.0218
$T = 1$	0.0558	0.1090	0.1091	0.1091	0.1091	0.1091
$T = 1.5$	0.0784	0.1771	0.1988	0.1989	0.1989	0.1989
$T = 2$	0.0972	0.2291	0.2689	0.2769	0.2769	0.2769
$T = 2.5$	0.1135	0.2735	0.3266	0.3413	0.3442	0.3442
$T = 3$	0.1282	0.3129	0.3773	0.3968	0.4020	0.4031

Table 2.2: Numerical results for $\tilde{V}(T, b)$ Contract I with recovery case

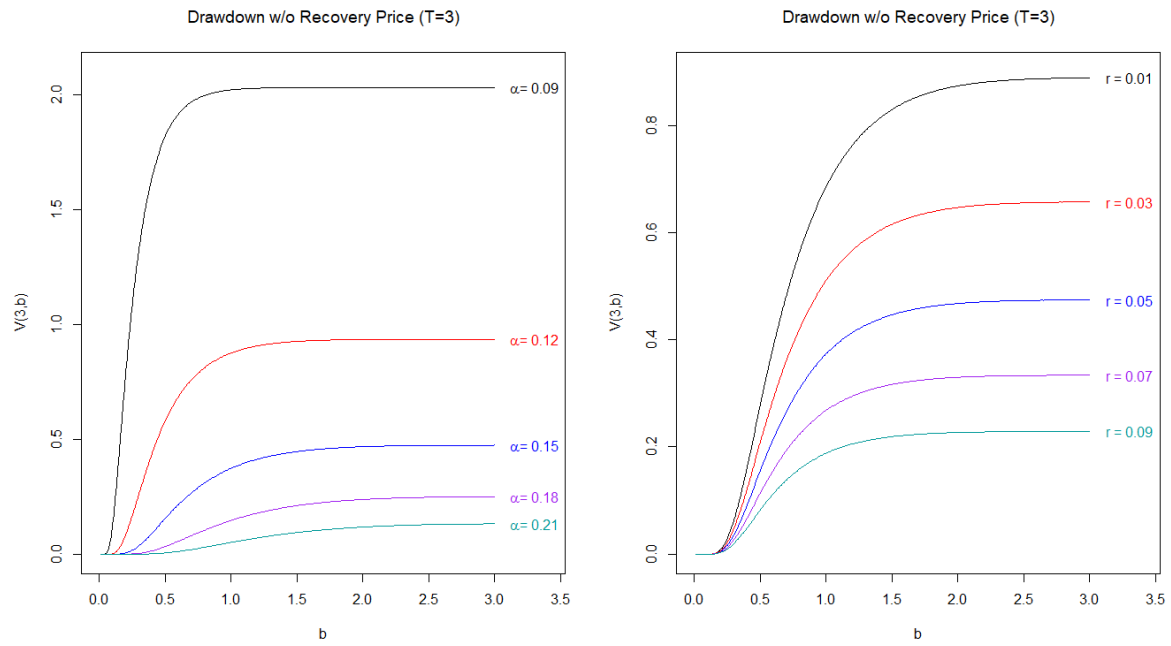
occur quickly enough, it will not result in a payoff. On the other hand, when $b \geq T$, the price converges. As discussed earlier, in this case the speed of market crash condition will satisfy almost surely whenever a drawdown occurs, so by dropping the market crash condition, our model reduces to the insurance on the frequency of drawdowns discussed in [12]. As such, the price of this product should be equal to that provided in Section 5 of [12]. When the threshold b exceeds the maturity time T , our results are indeed matched with those in Table 3 of [12]. Accuracy of this Laplace inversion estimation can be seen within four significant digits in most cases.

As the maturity T increases (for a fixed threshold b), the fair market value increases. This is because the longer the maturity, the more claims are possibly incurred.

Comparison between the fair market value of Contract I in both with and without recovery cases shows that the price without recovery is greater than those in the with recovery case. (When the maturity time T is too small, the differences are negligible.) This could be explained by the fact that the drawdown times with recovery are in a subset of the drawdown times without recovery. As drawdowns without recovery happen more often than drawdowns with recovery, it creates a higher price.

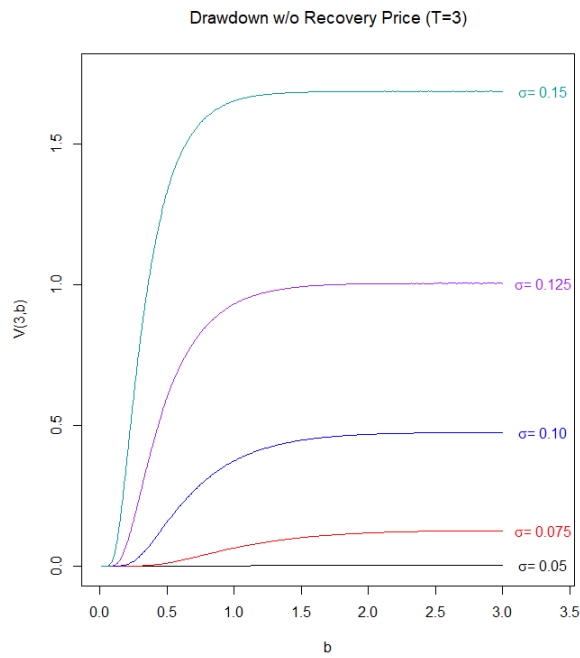
Now we conduct the sensitivity tests on the following parameters: the risk free rate r , drawdown size α , and volatility σ , for both insurance types (with and without recovery).

Figure 2.4 shows the sensitivity tests for Contract I without recovery case. In Figure 2.4, the maturity time is set to $T = 3$ years, and the fair market value is plotted as a function the speed of market crash threshold b under different choices of the parameter being tested. In each sub-figure, the fair market value is monotonically increasing function with respect to the threshold b until it reached the maturity time $T = 3$. This is expected since more drawdowns will be seen when the market crash constraint relaxes. When $b \geq T$, as discussed before, the



(a) For parameter α

(b) For parameter r



(c) For parameter σ

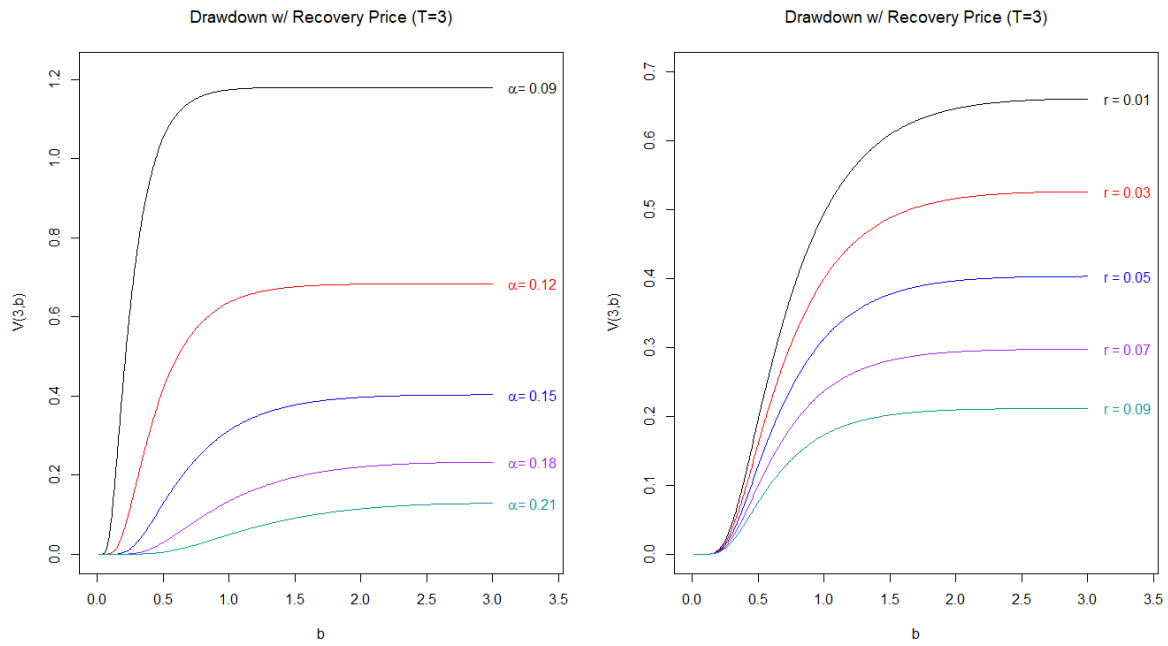
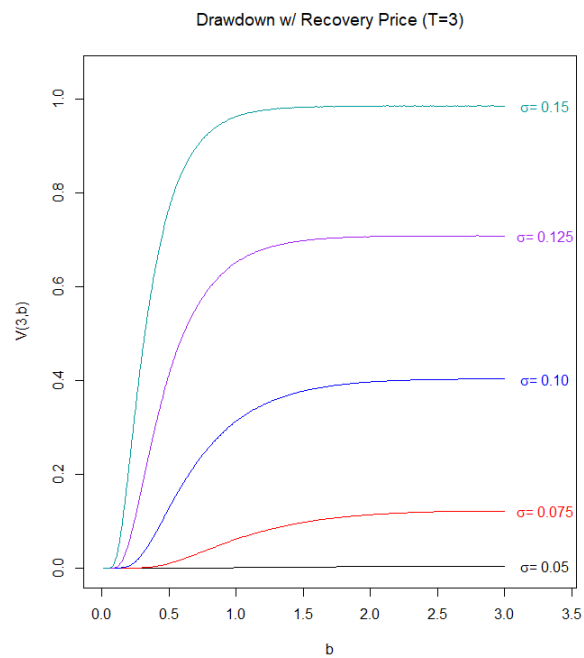
Figure 2.4: Sensitivity tests for $V(T, b)$ Contract I without recovery case

market crash constraint will be totally dropped. The price curve seems to flatten out even for some $b < T$, as it reaches the point where drawdowns will generally occur within the specified speed and the increases thereafter is very slow.

For a fixed threshold level b , we see that the fair market value are more sensitive to the parameters α and σ . In particular, we explain the observations as follows.

- In Figure 2.4 (a), the fair market value decreases quickly as the drawdown size α increases. This is a result of two facts: larger drawdowns are less likely to occur than smaller drawdowns, and larger drawdowns tend to have a slow speed of market crash as well.
- In Figure 2.4 (b), the fair market value decreases as the interest rate r increases. This could be explained by the discount factor dominating the drift of the BM.
- Figure 2.4 (c), the fair market value increases as the volatility σ increase, which means the more volatile of the underlying process, the more money needs to be charged to compensate the risk. When the volatility becomes small enough (or in this case, when $\sigma = 0.05$) we have a near flat price curve around 0. This is intuitive, as in this case, the opportunity for drawdowns to occur within a specific maturity period as well as speed of crash is extremely low.

Next we will look at the same sensitivity tests performed on Contract I with recovery case as illustrated in Figure 2.5. The graphs follow a similar pattern to those in the without recovery case. The price graphs under each scenario are lower than those in without recovery case. As mentioned previously, drawdowns without recovery occur as a subset of the drawdowns with recovery.

(a) For parameter α (b) For parameter r (c) For parameter σ Figure 2.5: Sensitivity tests for $\tilde{V}(T, b)$ Contract I with recovery case

Chapter 3

Knock-in Options on the Size of Drawdown Risk

In the previous chapter, we discussed the frequency and speed of drawdowns, as well as the valuation on their insurance products. It covers both with and without recovery cases, which provides some variability to the type of insurances that an investor can purchase, however the payoff at maturity considered was very basic — the digital payoff. In this chapter, we would like to examine the magnitude of drawdown risk and adapt the payoff based on the drawdown size of the underlying process to provide more versatile protection.

This chapter considers the fair market valuation of options regarding the drawdown risk, however with non-digital payoffs. In particular, our proposed options have payoffs depending on the (absolute or relative) size of the drawdown at maturity, given that a significant drawdown occurs prior to the maturity time as a knock-in feature. In other words, the knock-in is triggered when the maximum drawdown before maturity exceeds a prefixed threshold. We begin by discussing the model of interest and some preliminary results.

3.1 Model setup

In the valuation of the proposed drawdown option product, we assume that the underlying asset $\mathbb{S}_t = \{\mathbb{S}_t\}_{t \geq 0}$ is modeled by a geometric Brownian motion, whose dynamics under the risk-neutral measure \mathbb{Q} follows

$$d\mathbb{S}_t = r\mathbb{S}_t dt + \sigma\mathbb{S}_t dW_t^{\mathbb{Q}}, \quad \mathbb{S}_0 \in \mathbb{R}_+,$$

where $r \in \mathbb{R}_+$ is the risk free rate, $\sigma \in \mathbb{R}_+$ is the diffusion parameter, and $\{W_t^{\mathbb{Q}}\}_{t \geq 0}$ is a standard Brownian motion under the risk-neutral measure \mathbb{Q} .

This is the same model as discussed in Chapter 2, and as such, we use the same principals and relationships to allow us to work with the log-surplus process $X_t = \{X_t\}_{t \geq 0}$, where

$$X_t = \log(\mathbb{S}_t) = x + \mu t + \sigma W_t, \tag{3.1}$$

for $\mu, \sigma > 0$. In particular, we recall that the process X_t follows standard Brownian motion with drift $\mu := r - \frac{1}{2}\sigma^2$ and diffusion coefficient $\sigma \in \mathbb{R}_+$ under measure \mathbb{Q} , and its initial value $X_0 = x = \log \mathbb{S}_0$.

Using the same relationships between proportional and absolute drawdowns, we are able to complete the analysis of interested quantities using the drifted Brownian motion process $\{X_t\}$. In the following sections, all expectations and probabilities are under measure \mathbb{Q} , hence we will omit it for simplicity.

3.2 Preliminary results

In this section, we recall some results that are important for our valuation in the next section. We start from the general results in the spectrally negative Lévy process, and then simplify them in the drifted BM case.

3.2.1 Spectrally negative Lévy process

Consider a spectrally negative Lévy process $X = \{X_t\}_{t \geq 0}$ with the Laplace exponent $\psi(\lambda)$ and scale functions $W^{(q)}(x)$ and $Z^{(q)}(x)$ (see Chapter 1 for the definitions).

Lemma 3.2.1 *For $q \geq 0, y > 0$ and a spectrally negative Lévy process X , we have the following discounted density of the running maximum before drawdown*

$$\mathbb{E}_0(e^{-q\tau_D^+(a)} \cdot \mathbf{1}_{\{\bar{X}_{\tau_D^+(a)} \in dy\}}) = C^{(q)}(a) \cdot e^{-\rho^{(q)}(a)y} dy,$$

where the parameters $C^{(q)}(a)$ and $\rho^{(q)}(a)$ are given in terms of the scale functions

$$C^{(q)}(a) = \frac{Z^{(q)}(a)W^{(q),'}(a) - qW^{(q)}(a)^2}{W^{(q)}(a)},$$

and

$$\rho^{(q)}(a) = \frac{W^{(q),'}(a)}{W^{(q)}(a)}.$$

Proof We begin the proof by recalling Theorem 6.1 from [18] which has the result of the joint LTs

$$\mathbb{E}_0(e^{-\tau_D^+(a) - r g_{\tau_D^+(a)} - s D_{\tau_D^+(a)} - \delta \bar{X}_{\tau_D^+(a)}}) = \frac{W^{(q+r)}(a)}{\delta W^{(q+r)}(a) + W^{(q+r),'}(a)} \cdot \frac{Z_s^{(p)}(a)W_s^{(p),'}(a) - pW_s^{(p)}(a)^2}{W_s^{(p)}(a)}, \quad (3.2)$$

where $p = q - \Phi(s)$. When we set both $r = 0, s = 0$, we have

$$\mathbb{E}_0(e^{-q\tau_D^+(a) - \delta \bar{X}_{\tau_D^+(a)}}) = \frac{W^{(q)}(a)}{\delta W^{(q)}(a) + W^{(q),'}(a)} \frac{Z^{(q)}(a)W^{(q),'}(a) - qW^{(q)}(a)^2}{W^{(q)}(a)}. \quad (3.3)$$

Finally by taking the Laplace inversion w.r.t. δ , we complete the proof.

Let e_q be an independent exponential random variable with mean $1/q$. We also recall from Theorem 6.15(ii) of [9] the following lemma regarding the LTs of the running maximum and minimum at the independent exponential killing time (e_q) in the following lemma.

Lemma 3.2.2 *The LTs of the running maximum and minimum at the (independent) exponential killing time are given as*

$$\mathbb{E}_0(e^{-\beta\bar{X}_{e_q}}) = \frac{\Phi(q)}{\Phi(q) + \beta},$$

and

$$\mathbb{E}_0(e^{\beta X_{e_q}}) = \frac{q}{\Phi(q)} \frac{\beta - \Phi(q)}{\psi(\beta) - q}.$$

This means that \bar{X}_{e_q} is exponentially distributed with parameter $\Phi(q)$.

We also recall from Lemma 6.16 of [9] that the joint Laplace transform of (e_q, X_{e_q}) .

Lemma 3.2.3 *The Laplace transform of X_{e_q} at the (independent) exponential killing time (e_q) is given as*

$$\mathbb{E}_0(e^{-re_q + \beta X_{e_q}}) = \frac{q}{q + r - \psi(\beta)}.$$

Lastly, we consider the LT of the difference between the running maximum and the current value of the process, i.e., $\bar{X}_{e_q} - X_{e_q}$ in the following lemma.

Lemma 3.2.4 *For a spectrally negative Lévy process X , the Laplace transform of $\bar{X}_{e_q} - X_{e_q}$ is given as*

$$\mathbb{E}_0(e^{-\beta(\bar{X}_{e_q} - X_{e_q})}) = \frac{q}{\Phi(q)} \frac{\beta - \Phi(q)}{\psi(\beta) - q}.$$

Proof Using Equation (6.28) from [9], for $X_0 = 0$, the following two random variables are equal in distribution

$$(\bar{X}_{e_q} - X_{e_q}) \stackrel{d}{=} -\underline{X}_{e_q}.$$

Hence, from the second part of Lemma 3.2.2, we have

$$\mathbb{E}_0(e^{-\beta(\bar{X}_{e_q} - X_{e_q})}) = \mathbb{E}_0(e^{\beta X_{e_q}}) = \frac{q}{\Phi(q)} \frac{\beta - \Phi(q)}{\psi(\beta) - q}.$$

Note that for a general initial level $X_0 = y$, we can use a shift argument to generalize the above four lemmas to cover the expectations required for further calculation in next section.

1. For $z \geq y$,

$$\mathbb{E}_y(e^{-q\tau_D^+(a)} \cdot \mathbf{1}_{\{\bar{X}_{\tau_D^+(a)} \in dy\}}) = C^{(q)}(a) \cdot e^{-\rho^{(q)}(a)(z-y)} dz, \quad (3.4)$$

2. The discounted LT of the running maximum at e_q is

$$\mathbb{E}_y(e^{-re_q - \beta\bar{X}_{e_q}}) = e^{-\beta y} \frac{q}{q + r} \frac{\Phi(q)}{\Phi(q) + \beta}, \quad (3.5)$$

since making use of the independence assumption of e_q ,

$$\begin{aligned}
\mathbb{E}_y\left(e^{-re_q - \beta \bar{X}_{e_q}}\right) &= q \int_0^\infty e^{-qt} \mathbb{E}_y(e^{-rt} e^{-\beta \bar{X}_t}) dt \\
&= q \int_0^\infty e^{-(q+r)t} \mathbb{E}_y(e^{-\beta \bar{X}_t}) dt \\
&= \frac{q}{q+r} \int_0^\infty (q+r) e^{-(q+r)t} \mathbb{E}_y(e^{-\beta \bar{X}_t}) dt \\
&= \frac{q}{q+r} \mathbb{E}_y(e^{-\beta \bar{X}_{e_{q+r}}}) \\
&= \frac{q}{q+r} e^{-\beta y} \mathbb{E}_0(e^{-\beta \bar{X}_{e_{q+r}}}).
\end{aligned}$$

3. The discounted LT of the surplus level at e_q is

$$\mathbb{E}_y(e^{-re_q + \beta X_{e_q}}) = e^{\beta y} \mathbb{E}_0(e^{-re_q + \beta X_{e_q}}) = e^{\beta y} \frac{q}{q+r - \psi(\beta)}. \quad (3.6)$$

4. Note that the result in Lemma 3.2.4 is independent of the initial level $X_0 = y$, and we can further involve the time discounting as

$$\mathbb{E}_y(e^{-re_q - \beta(\bar{X}_{e_q} - X_{e_q})}) = \frac{q}{\Phi(q+r)} \frac{\beta - \Phi(q+r)}{\psi(\beta) - (q+r)}, \quad (3.7)$$

whose derivation is similar to Equation (3.5).

3.2.2 Drifted BM

For the drifted BM, the Laplace exponent is

$$\psi(s) = \frac{1}{2} \sigma^2 s^2 + \mu s.$$

Since we know the LT of $W^{(q)}(x)$ is given as in (1.16), we can take the LT inversion w.r.t. s to find the function of $W^{(q)}(x)$ explicitly. Letting $\delta = \frac{\mu}{\sigma^2}$ and $\gamma_q = \sqrt{\delta^2 + \frac{2q}{\sigma^2}}$, we have

$$W^{(q)}(x) = \frac{2}{\sigma^2 \gamma_q} e^{-\delta x} \sinh(\gamma_q x) = \frac{1}{\sigma^2 \gamma_q} \left(e^{-(\delta - \gamma_q)x} - e^{-(\delta + \gamma_q)x} \right), \quad (3.8)$$

for $x \geq 0$, where $\sinh(x) = \frac{e^x - e^{-x}}{2}$, and $W^{(q)}(x) = 0$ when $x < 0$.

The second scale function $Z^{(q)}(x)$ is then equal to

$$Z^{(q)}(x) = 1 + q \int_0^x W^{(q)}(y) dy = \frac{q}{\sigma^2 \gamma_q} \left(\frac{e^{-(\delta + \gamma_q)x}}{\delta + \gamma_q} - \frac{e^{-(\delta - \gamma_q)x}}{\delta - \gamma_q} \right).$$

Given the $W^{(q)}(x)$ function above, we can find its derivation as

$$W^{(q),\prime}(x) = -\frac{1}{\sigma^2 \gamma_q} \left((\delta - \gamma_q) e^{-(\delta - \gamma_q)x} - (\delta + \gamma_q) e^{-(\delta + \gamma_q)x} \right), \quad (3.9)$$

and therefore we can see that $C^{(q)}(a)$ and $\rho^{(q)}(a)$ can be simply found as

$$\begin{aligned} C^{(q)}(a) &= \frac{Z^{(q)}(a)W^{(q)'}(a) - qW^{(q)}(a)^2}{W^{(q)}(a)} \\ &= \frac{\frac{q}{(\sigma^2\gamma_q)^2} \frac{(2\gamma_q)^2}{2q/\sigma^2} e^{-2\delta a}}{\frac{1}{\sigma^2\gamma_q} (e^{-(\delta-\gamma_q)a} - e^{-(\delta+\gamma_q)a})} \\ &= \frac{\frac{2}{\sigma^2} e^{-2\delta a}}{\frac{1}{\sigma^2\gamma_q} (e^{-(\delta-\gamma_q)a} - e^{-(\delta+\gamma_q)a})} \\ &= \frac{2\gamma_q e^{-(\delta+\gamma_q)a}}{1 - e^{-2\gamma_q a}}, \end{aligned}$$

and

$$\rho^{(q)}(a) = \frac{W^{(q)'}(a)}{W^{(q)}(a)} = \frac{(\delta + \gamma_q)e^{-2\gamma_q a} - (\delta - \gamma_q)}{1 - e^{-2\gamma_q a}} = \frac{\gamma_q(1 + e^{-2\gamma_q a})}{1 - e^{-2\gamma_q a}} - \delta. \quad (3.10)$$

3.3 The valuation of knock-in drawdown options

We propose a knock-in drawdown option, which has the payoff of P_T at maturity time T if a significant of proportional drawdown of size α occurs before maturity, and the payoff is 0 otherwise

$$\text{payoff at time } T = P_T 1_{\{T_S^+(\alpha) < T\}}.$$

The fair market value at time 0, denoted as $V(T)$ (a function of maturity time T), is then given by

$$V(T) = \mathbb{E}\left(e^{-rT} P_T 1_{\{T_S^+(\alpha) < T\}}\right). \quad (3.11)$$

Other than the digital \$1 payoff, we consider the following two types of payoffs which depends on the size of drawdown:

- **Type I:** the payoff depends on the absolute drawdown at maturity, i.e.,

$$P_T = \bar{\mathbb{S}}_T - \mathbb{S}_T,$$

thus the fair market value is denoted

$$V_1(T) := \mathbb{E}\left[e^{-rT} (\bar{\mathbb{S}}_T - \mathbb{S}_T) 1_{\{T_S^+(\alpha) < T\}}\right],$$

or equivalently, by using the process $\{X_t\}$,

$$V_1(T) = \mathbb{E}_x\left[e^{-rT} (e^{\bar{X}_T} - e^{X_T}) 1_{\{\tau_D^+(a) < T\}}\right]. \quad (3.12)$$

Note that we add the subscript x for the expectation because it depends on the initial value $X_0 = x$.

- **Type II:** the payoff depends on the proportional drawdown at maturity

$$P_T = \frac{\bar{S}_T}{S_T},$$

whose fair market value is denoted as

$$V_2(T) := \mathbb{E}\left[e^{-rT} \left(\frac{\bar{S}_T}{S_T}\right) \mathbf{1}_{\{T_S^+(a) < T\}}\right] = \mathbb{E}\left[e^{-rT} \left(e^{\bar{X}_T - X_T}\right) \mathbf{1}_{\{\tau_D^+(a) < T\}}\right].$$

Note that this expectation is independent of the initial value $X_0 = x$.

The pricing for these two types of options are given in the following two theorems.

Theorem 3.3.1 *For $r > 0$ and the process X follows a drifted BM as in (3.1), the LT of the fair market price for Type I option is given as*

$$\int_0^\infty e^{-qT} V_1(T) dT = \frac{C^{(q+r)}(a)}{(q+r)(\rho^{(q+r)}(a) - 1)} \left[1 + \frac{e^{-\Phi(q+r)a}}{\Phi(q+r) - 1} - \frac{(q+r)e^{-a}}{q+r - \psi(1)} \right] e^x.$$

where r is the constant force of interest, and other parameters are given in Section 3.2.1.

Proof Here we use the LT transform technique (or the technique of randomization or Canadization), i.e.,

$$\begin{aligned} q \int_0^\infty e^{-qT} V_1(T) dT &= q \int_0^\infty e^{-qT} \mathbb{E}_x \left[e^{-rT} P_T \mathbf{1}_{\{\tau_D^+(a) < T\}} \right] dT \\ &= \mathbb{E}_x \left[e^{-re_q} P_{e_q} \mathbf{1}_{\{\tau_D^+(a) < e_q\}} \right], \end{aligned}$$

where recall that e_q follows an independent exponential random variable with mean $1/q$. By using Canadization and letting $T = e_q$, we could use the memoryless property to simplify the derivation as

$$e_q - z \mid e_q > z \stackrel{d}{=} e_q.$$

We begin by separating the expectation into two cases depending on whether e_q occurs before or after recovery. We define T_1 as the time at which the process X recovers to the maximum \bar{X} , as such

$$T_1 = \tau_D^+(a) \circ \tau_X^+(a),$$

which can occur either before or after the random time e_q . This allows us to separate the expectation as follows

$$\mathbb{E}_x \left(e^{-re_q} P_{e_q} \cdot \mathbf{1}_{\{\tau_D^+(a) < e_q\}} \right) = \mathbb{E}_x \left(e^{-re_q} P_{e_q} \cdot \mathbf{1}_{\{\tau_D^+(a) < e_q, T_1 < e_q\}} \right) + \mathbb{E}_x \left(e^{-re_q} P_{e_q} \cdot \mathbf{1}_{\{\tau_D^+(a) < e_q, T_1 > e_q\}} \right) := DDP^{(1)} + DDP^{(2)}. \quad (3.13)$$

It is important to note that the reason we are interested in whether the process recovers or not, even though we are only considering a single drawdown event, is that the payoff is dependent on the drawdown size. As such, if the process recovers, the payoff will differ due to the change in the maximum of X and be priced differently.

For both cases — with recovery ($DDP^{(1)}$) and without recovery ($DDP^{(2)}$) — we will use the renewal argument as follows.

By conditioning on the drawdown time and the running maximum before drawdown, we make use of the strong Markov property of X and it gives

$$\begin{aligned}
DDP^{(1)} &= \mathbb{E}_x \left(\mathbb{E} \left(e^{-re_q} P_{e_q} \cdot \mathbf{1}_{\{\tau_D^+(a) < e_q, T_1 < e_q\}} \middle| \mathcal{F}_{\tau_D^+(a)} \right) \right) \\
&= \mathbb{E}_x \left(e^{-(r+q)\tau_D^+(a)} \cdot \mathbb{E}_{X_{\tau_D^+(a)}} \left(e^{-re_q} P_{e_q} \cdot \mathbf{1}_{\{\tau_X^+(\bar{X}_{\tau_D^+(a)}) < e_q\}} \right) \right) \\
&= \int_x^\infty \mathbb{E}_x \left(e^{-(r+q)\tau_D^+(a)} \cdot \mathbf{1}_{\{\bar{X}_{\tau_D^+(a)} \in dy\}} \right) \cdot \mathbb{E}_{y-a} \left(e^{-re_q} P_{e_q} \cdot \mathbf{1}_{\{\tau_X^+(y) < e_q\}} \right) \\
&= \int_x^\infty \mathbb{E}_x \left(e^{-(r+q)\tau_D^+(a)} \cdot \mathbf{1}_{\{\bar{X}_{\tau_D^+(a)} \in dy\}} \right) \cdot \mathbb{E}_{y-a} \left(\mathbb{E} \left(e^{-re_q} P_{e_q} \cdot \mathbf{1}_{\{\tau_X^+(y) < e_q\}} \middle| \tau_X^+(y) \right) \right) \\
&= \int_x^\infty \mathbb{E}_x \left(e^{-(r+q)\tau_D^+(a)} \cdot \mathbf{1}_{\{\bar{X}_{\tau_D^+(a)} \in dy\}} \right) \cdot \mathbb{E}_{y-a} \left(e^{-r\tau_X^+(y)} \mathbf{1}_{\{\tau_X^+(y) < e_q\}} \cdot \mathbb{E}_{X_{\tau_X^+(y)}} \left(e^{-re_q} P_{e_q} \right) \right) \\
&= \int_x^\infty \mathbb{E}_x \left(e^{-(r+q)\tau_D^+(a)} \cdot \mathbf{1}_{\{\bar{X}_{\tau_D^+(a)} \in dy\}} \right) \cdot \mathbb{E}_{y-a} \left(e^{-(r+q)\tau_X^+(y)} \right) \cdot \mathbb{E}_y \left(e^{-re_q} P_{e_q} \right), \tag{3.14}
\end{aligned}$$

where after recovering to the previous running maximum, the term $\mathbb{E}_y \left(e^{-re_q} P_{e_q} \right)$ represents a traditional look-back option with payoff of the absolute drawdown at (the randomized) maturity with

$$\mathbb{E}_y \left(e^{-re_q} P_{e_q} \right) = \mathbb{E}_y \left(e^{-re_q} \left(e^{\bar{X}_{e_q}} - e^{X_{e_q}} \right) \right) = \frac{q}{q+r} e^y \left(\frac{\Phi(q+r)}{\Phi(q+r)-1} - \frac{q+r}{q+r-\psi(1)} \right),$$

using Equations (3.5) and (3.6).

Thus, we can further substitute the first two expectations in (3.14) using the results of Lemmas 3.2.1 and 2.3.2 respectively. We obtain the following result

$$\begin{aligned}
DDP^{(1)} &= \int_x^\infty C^{(q+r)}(a) e^{-\rho^{(q+r)}(a)(y-x)} e^{-\Phi(q+r)a} \frac{q}{q+r} e^y \left(\frac{\Phi(q+r)}{\Phi(q+r)-1} - \frac{q+r}{q+r-\psi(1)} \right) dy \\
&= C^{(q+r)}(a) e^{-\Phi(q+r)a} \frac{q}{q+r} \left(\frac{\Phi(q+r)}{\Phi(q+r)-1} - \frac{q+r}{q+r-\psi(1)} \right) e^{\rho^{(q+r)}(a)x} \int_x^\infty e^{-\rho^{(q+r)}(a)(a-1)y} dy \\
&= C^{(q+r)}(a) e^{-\Phi(q+r)a} \frac{q}{q+r} \left(\frac{\Phi(q+r)}{\Phi(q+r)-1} - \frac{q+r}{q+r-\psi(1)} \right) \frac{e^x}{\rho^{(q+r)}(a)-1}.
\end{aligned}$$

This completes the calculation for $DDP^{(1)}$.

Now we move to $DDP^{(2)}$. If the running maximum is not recovered, by conditioning on the drawdown time and the running maximum before drawdown, we have

$$\begin{aligned}
DDP^{(2)} &= \mathbb{E}_x \left(\mathbb{E} \left(e^{-re_q} P_{e_q} \cdot \mathbf{1}_{\{\tau_D^+(a) < e_q, T_1 > e_q\}} \middle| \mathcal{F}_{\tau_D^+(a)} \right) \right) \\
&= \mathbb{E}_x \left(e^{-r\tau_D^+(a)} \mathbf{1}_{\{\tau_D^+(a) < e_q\}} \cdot \mathbb{E}_{X_{\tau_D^+(a)}} \left(e^{-re_q} P_{e_q} \cdot \mathbf{1}_{\{\tau_X^+(\bar{X}_{\tau_D^+(a)}) > e_q\}} \right) \right) \\
&= \int_x^\infty \mathbb{E}_x \left(e^{-(r+q)\tau_D^+(a)} \cdot \mathbf{1}_{\{\bar{X}_{\tau_D^+(a)} \in dy\}} \right) \cdot \mathbb{E}_{y-a} \left(e^{-re_q} P_{e_q} \cdot \mathbf{1}_{\{\tau_X^+(y) > e_q\}} \right) \\
&= \int_x^\infty \mathbb{E}_x \left(e^{-(r+q)\tau_D^+(a)} \cdot \mathbf{1}_{\{\bar{X}_{\tau_D^+(a)} \in dy\}} \right) \cdot \mathbb{E}_{y-a} \left(e^{-re_q} \left(e^y - e^{X_{e_q}} \right) \cdot \mathbf{1}_{\{\tau_X^+(y) > e_q\}} \right), \tag{3.15}
\end{aligned}$$

where the last step is because of the the payoff function $P_T = e^{\bar{X}_T} - e^{X_T}$, and the current running maximum is at level y . Furthermore, we can decompose the second term in (3.15) as (for simplicity, we will denote this term as $DDP_2^{(2)}$)

$$\begin{aligned}
DDP_2^{(2)} &:= \mathbb{E}_{y-a} \left(e^{-re_q} (e^y - e^{X_{e_q}}) \cdot 1_{\{\tau_X^+(y) > e_q\}} \right) \\
&= \mathbb{E}_{y-a} \left(e^{-re_q} e^y \cdot 1_{\{\tau_X^+(y) > e_q\}} \right) - \mathbb{E}_{y-a} \left(e^{-re_q} e^{X_{e_q}} \cdot 1_{\{\tau_X^+(y) > e_q\}} \right) \\
&= e^y \frac{q}{q+r} \mathbb{E}_{y-a} \left(1 - e^{-(q+r)\tau_X^+(y)} \right) - \left(\mathbb{E}_{y-a} \left(e^{-re_q} e^{X_{e_q}} \right) - \mathbb{E}_{y-a} \left(e^{-re_q} e^{X_{e_q}} \cdot 1_{\{\tau_X^+(y) < e_q\}} \right) \right) \\
&= e^y \frac{q}{q+r} \left(1 - \mathbb{E}_{y-a} [e^{-(q+r)\tau_X^+(y)}] \right) - \left(\mathbb{E}_{y-a} \left(e^{-re_q} e^{X_{e_q}} \right) - \mathbb{E}_{y-a} \left(e^{-(r+q)\tau_X^+(y)} \right) \cdot \mathbb{E}_y \left(e^{-re_q} e^{X_{e_q}} \right) \right),
\end{aligned}$$

Again, by making use of Equation (3.6) and Lemma 2.3.2, we have

$$\begin{aligned}
DDP_2^{(2)} &= e^y \frac{q}{q+r} \left(1 - e^{-\Phi(q+r)a} \right) - \left[e^{y-a} \frac{q}{q+r} \frac{q+r}{q+r-\psi(1)} - e^{-\Phi(q+r)a} e^y \frac{q}{q+r} \frac{q+r}{q+r-\psi(1)} \right] \\
&= e^y \frac{q}{q+r} \left[1 - e^{-\Phi(q+r)a} - (e^{-a} - e^{-\Phi(q+r)a}) \frac{q+r}{q+r-\psi(1)} \right].
\end{aligned}$$

Thus, substituting the calculation back into Equation (3.15) and using Lemma 3.2.1, we have

$$\begin{aligned}
DDP^{(2)} &= \int_x^\infty C^{(q+r)}(a) e^{-\rho^{(q+r)}(a)(y-x)} e^y \frac{q}{q+r} \left[1 - e^{-\Phi(q+r)a} - (e^{-a} - e^{-\Phi(q+r)a}) \frac{q+r}{q+r-\psi(1)} \right] dy \\
&= C^{(q+r)}(a) \frac{q}{q+r} \left[1 - e^{-\Phi(q+r)a} - (e^{-a} - e^{-\Phi(q+r)a}) \frac{q+r}{q+r-\psi(1)} \right] \frac{e^x}{\rho^{(q+r)}(a) - 1}.
\end{aligned}$$

Finally, by adding $DDP^{(1)}$ and $DDP^{(2)}$ together,

$$\begin{aligned}
&q \int_0^\infty e^{-qT} V_1(T) dT = DDP^{(1)} + DDP^{(2)} \\
&= C^{(q+r)}(a) e^{-\Phi(q+r)a} \frac{q}{q+r} \left(\frac{\Phi(q+r)}{\Phi(q+r)-1} - \frac{q+r}{q+r-\psi(1)} \right) \frac{e^x}{\rho^{(q+r)}(a) - 1} \\
&\quad + C^{(q+r)}(a) \frac{q}{q+r} \left[1 - e^{-\Phi(q+r)a} - (e^{-a} - e^{-\Phi(q+r)a}) \frac{q+r}{q+r-\psi(1)} \right] \frac{e^x}{\rho^{(q+r)}(a) - 1} \\
&= \frac{q}{q+r} C^{(q+r)}(a) \frac{e^x}{\rho^{(q+r)}(a) - 1} \left[1 + e^{-\Phi(q+r)a} \frac{1}{\Phi(q+r)-1} - e^{-a} \frac{q+r}{q+r-\psi(1)} \right],
\end{aligned}$$

which completes the proof.

Now we present the main result for the Type II option.

Theorem 3.3.2 *For $r > 0$ and the process X follows a drifted BM as in (3.1), the LT of the fair market price for Type II option is given as*

$$\int_0^\infty e^{-qT} V_2(T) dT = \frac{C^{(q+r)}(a) e^a + \frac{1}{\Phi(q+r)} e^{-\Phi(q+r)a}}{\rho^{(q+r)}(a) \frac{q+r-\psi(-1)}{q+r-\psi(1)}}. \quad (3.16)$$

Proof The proof of this theorem can be done in a similar way as Theorem 3.3.1 by separating the expectation into $DDP^{(1)}$ and $DDP^{(2)}$, depending on whether e_q happens before or after recovery. However, we need to incorporate the new payoff for this Type II product. Similarly we could consider the LT of $V_2(T)$ and recall Equation (3.13) that

$$\begin{aligned} q \int_0^\infty e^{-qT} V_2(T) dT &= \mathbb{E}_x \left[e^{-re_q} P_{e_q} \mathbf{1}_{\{\tau_D^+(a) < e_q\}} \right] \\ &= \mathbb{E}_x \left(e^{-re_q} P_{e_q} \cdot \mathbf{1}_{\{\tau_D^+(a) < e_q, T_1 < e_q\}} \right) + \mathbb{E}_x \left(e^{-re_q} P_{e_q} \cdot \mathbf{1}_{\{\tau_D^+(a) < e_q, T_1 > e_q\}} \right) \\ &:= DDP^{(1)} + DDP^{(2)}, \end{aligned}$$

where with the type II payoff function is given as $P_t = e^{\bar{X}_t - X_t}$.

By conditioning on the drawdown time and the running maximum before drawdown, we make use of the strong Markov property of X and it gives

$$\begin{aligned} DDP^{(1)} &= \int_x^\infty \mathbb{E}_x \left(e^{-(r+q)\tau_D^+(a)} \cdot \mathbf{1}_{\{\bar{X}_{\tau_D^+(a)} \in dy\}} \right) \cdot \mathbb{E}_{y-a} \left(e^{-(r+q)\tau_X^+(y)} \right) \cdot \mathbb{E}_y \left(e^{-re_q} P_{e_q} \right) \\ &= \int_x^\infty C^{(q+r)}(a) e^{-\rho^{(q+r)}(a)(y-x)} e^{-\Phi(q+r)a} \frac{q}{\Phi(q+r)} \frac{\Phi(q+r) + 1}{(q+r) - \psi(-1)} dy \\ &= \frac{C^{(q+r)}(a)}{\rho^{(q+r)}(a)} e^{-\Phi(q+r)a} \frac{q}{\Phi(q+r)} \frac{\Phi(q+r) + 1}{q+r - \psi(-1)}, \end{aligned}$$

where we have

$$\mathbb{E}_y \left(e^{-re_q} P_{e_q} \right) = \mathbb{E}_y \left(e^{-re_q} e^{\bar{X}_{e_q} - X_{e_q}} \right) = \frac{q}{\Phi(q+r)} \frac{\Phi(q+r) + 1}{q+r - \psi(-1)},$$

using Equations (3.7). This completes the calculation for $DDP^{(1)}$.

Now we move to $DDP^{(2)}$. If the running maximum is not recovered, by conditioning on the drawdown time and the running maximum before drawdown, we have

$$\begin{aligned} DDP^{(2)} &= \int_x^\infty \mathbb{E}_x \left(e^{-(r+q)\tau_D^+(a)} \cdot \mathbf{1}_{\{\bar{X}_{\tau_D^+(a)} \in dy\}} \right) \cdot \mathbb{E}_{y-a} \left(e^{-re_q} P_{e_q} \cdot \mathbf{1}_{\{\tau_X^+(y) > e_q\}} \right) \\ &= \int_x^\infty \mathbb{E}_x \left(e^{-(r+q)\tau_D^+(a)} \cdot \mathbf{1}_{\{\bar{X}_{\tau_D^+(a)} \in dy\}} \right) \cdot \mathbb{E}_{y-a} \left(e^{-re_q} (e^{y-X_{e_q}}) \cdot \mathbf{1}_{\{\tau_X^+(y) > e_q\}} \right), \end{aligned}$$

where the second part in the integration can be calculated as

$$\begin{aligned} &\mathbb{E}_{y-a} \left(e^{-re_q} (e^{y-X_{e_q}}) \cdot \mathbf{1}_{\{\tau_X^+(y) > e_q\}} \right) \\ &= \mathbb{E}_0 \left(e^{-re_q} (e^{a-X_{e_q}}) \cdot \mathbf{1}_{\{\tau_X^+(a) > e_q\}} \right) \\ &= e^a \left(\mathbb{E}_0 \left(e^{-re_q} e^{-X_{e_q}} \right) - \mathbb{E}_0 \left(e^{-re_q} e^{-X_{e_q}} \cdot \mathbf{1}_{\{\tau_X^+(a) < e_q\}} \right) \right) \\ &= e^a \left(\mathbb{E}_0 \left(e^{-re_q} e^{-X_{e_q}} \right) - \mathbb{E}_0 \left(e^{-(r+q)\tau_X^+(a)} \right) \cdot \mathbb{E}_a \left(e^{-re_q} e^{-X_{e_q}} \right) \right) \\ &= e^a \left(\frac{q}{q+r - \psi(-1)} - e^{-\Phi(q+r)a} e^{-a} \frac{q}{q+r - \psi(-1)} \right) \\ &= \frac{q}{q+r - \psi(-1)} \left(e^a - e^{-\Phi(q+r)a} \right), \end{aligned}$$

using Equation (3.6).

Thus, substituting this back to the $DDP^{(2)}$ and together with Lemma 3.2.1, we have

$$\begin{aligned} DDP^{(2)} &= \int_x^\infty C^{(q+r)}(a) e^{-\rho^{(q+r)}(a)(y-x)} \frac{q}{q+r-\psi(-1)} (e^a - e^{-\Phi(q+r)a}) dy \\ &= \frac{C^{(q+r)}(a)}{\rho^{(q+r)}(a)} \frac{q}{q+r-\psi(-1)} (e^a - e^{-\Phi(q+r)a}). \end{aligned}$$

Finally, by adding $DDP^{(1)}$ and $DDP^{(2)}$ together,

$$\begin{aligned} q \int_0^\infty e^{-qT} V_2(T) dT &= DDP^{(1)} + DDP^{(2)} \\ &= \frac{C^{(q+r)}(a)}{\rho^{(q+r)}(a)} e^{-\Phi(q+r)a} \frac{q}{\Phi(q+r)} \frac{\Phi(q+r)+1}{q+r-\psi(-1)} + \frac{C^{(q+r)}(a)}{\rho^{(q+r)}(a)} \frac{q}{q+r-\psi(-1)} (e^a - e^{-\Phi(q+r)a}) \\ &= \frac{q}{q+r-\psi(-1)} \frac{C^{(q+r)}(a)}{\rho^{(q+r)}(a)} \left[e^a + \frac{1}{\Phi(q+r)} e^{-\Phi(q+r)a} \right], \end{aligned}$$

which completes the proof.

3.4 Connections with the existing models

3.4.1 Connection with lookback put option

When $a = 0$, $\tau_D^+(a) < T$ almost surely. In this case, the Type I contract reduces to the lookback put option with a floating strike rate

$$V_u(T) := V_1(T)|_{a=0} = \mathbb{E} \left(e^{-rT} (\bar{\mathbb{S}}_T - \mathbb{S}_T) \right),$$

where we denote this value as $V_u(T)$ because this provides an upper bound for $V_1(T)$.

From Theorem 3.3.1, the LT of $V_u(T)$ is given as (with $a = 0$)

$$\begin{aligned} \int_0^\infty e^{-qT} V_u(T) dT &= \mathbb{S}_0 \frac{C^{(q+r)}(0)}{(q+r)(\rho^{(q+r)}(0) - 1)} \left[1 + \frac{1}{\Phi(q+r) - 1} - \frac{q+r}{q+r-\psi(1)} \right] \\ &= \mathbb{S}_0 \left(\frac{1}{q+r} \frac{\Phi(q+r)}{\Phi(q+r) - 1} - \frac{1}{q} \right), \end{aligned} \tag{3.17}$$

where we use the following results in the simplification

$$\frac{C^{(q+r)}(0)}{\rho^{(q+r)}(0) - 1} = \lim_{a \rightarrow 0} \frac{C^{(q+r)}(a)}{\rho^{(q+r)}(a) - 1} = 1,$$

and

$$\psi(1) = \mu + \frac{\sigma^2}{2} = r.$$

A well-known result for the lookback put option price with a fixed maturity time T , denoted as $\hat{V}_u(T)$, is

$$\hat{V}_u(T) = M_0 e^{-rT} N(-d_1 + \sigma \sqrt{T}) - \mathbb{S}_0 N(-d_1) + e^{-rT} \frac{\sigma^2}{2r} \mathbb{S}_0 \left(e^{rT} N(d_1) - \left(\frac{\mathbb{S}_0}{M_0} \right)^{-\frac{2r}{\sigma^2}} N(d_1 - \frac{2r}{\sigma} \sqrt{T}) \right),$$

where $M_0 = \bar{\mathbb{S}}_0$ and

$$d_1 = \frac{\log(\mathbb{S}_0/M_0) + (r + \sigma^2/2)T}{\sigma \sqrt{T}}.$$

Actually we can show that, when $\bar{\mathbb{S}}_0 = \mathbb{S}_0$, the LT of $\hat{V}_u(T)$ is same as in (3.17), i.e.,

$$\int_0^\infty e^{-qT} \hat{V}_u(T) dT = \int_0^\infty e^{-qT} V_u(T) dT, \quad (3.18)$$

therefore, due to the uniqueness of LT, we have

$$\hat{V}_u(T) = V_u(T).$$

In other words, in the case of $a = 0$, our main result is consistent with the valuation of the lookback put option with a floating strike, which provides an upper bound for our knock-in option with Type I payoff on drawdown risk. For conciseness, we postpone the proof of Equation (3.18) to the Appendix A.

3.4.2 Connection with digital option on maximum drawdown

To build the connection with digital option, we will first generalize the Type II payoff by adding a parameter β to raise to the power as

$$P_T^\beta = \left(\frac{\bar{\mathbb{S}}_T}{\mathbb{S}_T} \right)^\beta,$$

which has the valuation function

$$V_2^\beta(T) := \mathbb{E} \left[e^{-rT} \left(\frac{\bar{\mathbb{S}}_T}{\mathbb{S}_T} \right)^\beta 1_{\{\tau_D^+(a) < T\}} \right] = \mathbb{E} \left[e^{-rT} e^{\beta(\bar{X}_T - X_T)} 1_{\{\tau_D^+(a) < T\}} \right]. \quad (3.19)$$

Hence the relationship with the original Type II payoff contract is $V_2(T) = V_2^\beta(T)|_{\beta=1}$.

Note that this parameter does not add any calculation complex in the proof of Theorem 3.3.2, and one can easily follow the same step to obtain the following result

$$\int_0^\infty e^{-qT} V_2^\beta(T) dT = \frac{1}{q+r-\psi(-\beta)} \frac{C^{(q+r)}(a)}{\rho^{(q+r)}(a)} \left[e^{\beta a} + \frac{\beta}{\Phi(q+r)} e^{-\Phi(q+r)a} \right]. \quad (3.20)$$

The proof of Equation (3.20) is postponed to Appendix B.

When $\beta = 0$,

$$V_2^\beta(T)|_{\beta=0} = \mathbb{E} \left[e^{-rT} 1_{\{\tau_D^+(a) < T\}} \right] = \mathbb{E} \left[e^{-rT} 1_{\{\bar{D}_T \geq a\}} \right],$$

it reduces to the digital call option on maximum drawdown, whose LT becomes

$$\int_0^\infty e^{-qT} V_2^\beta(T)|_{\beta=0} dT = \frac{1}{q+r} \frac{C^{(q+r)}(a)}{\rho^{(q+r)}(a)}. \quad (3.21)$$

This digital call option could serve as a lower bound for our Type II payoff contract $V_2(T)$.

Note that Equation (3.21) can also be seen as

$$\mathbb{E} \left[e^{-re_q} 1_{\{\tau_D^+(a) < e_q\}} \right] = \frac{1}{q+r} \mathbb{E} \left[e^{-(q+r)\tau_D^+(a)} \right] = \frac{1}{q+r} \frac{C^{(q+r)}(a)}{\rho^{(q+r)}(a)},$$

from Lemma 3.2.1.

3.5 Numerical results

In this section, we will give numerical results from the theoretical results in the previous section that are given in their Laplace transforms. To find the price analytically, we need to complete the LT inversion of the function. However, due to the complexity of the expressions, in this section we will complete the LT inversion numerically; see Section 1.4 for more information. In particular, we will adopt the Talbot algorithm given as

$$\mathcal{T}(M) := f_b(t, M) = \frac{2}{5t} \sum_{k=0}^{M-1} \operatorname{Re} \left(\gamma_k \tilde{f} \left(\frac{\delta_k}{t} \right) \right),$$

where

$$\delta_0 = \frac{2M}{5}, \quad \delta_k = \frac{2k\pi}{5} (\cot(k\pi/M) + i), \quad 0 < k < M,$$

$$\gamma_0 = \frac{1}{2} e^{\delta_0}, \quad \gamma_k = [1 + i(k\pi/M)(1 + [\cot(k\pi/M)]^2) - i \cot(k\pi/M)] e^{\delta_k}, \quad 0 < k < M.$$

3.5.1 Type I option

In this section, we work towards numerically inverting our results in Theorem 3.3.1, i.e., the Type I option. We will need to conduct the Laplace inversion with respect to the Laplace argument q . In the numerical example, we set the parameters for this inversion as follows:

- the risk-free rate $r = 0.05$
- absolute drawdown size $a = 0.15$, or equivalently $\alpha = 1 - e^{-a}$
- the volatility $\sigma = 0.10$
- the initial value $\mathbb{S}_0 = 100$, or equivalently $X_0 = \log(\mathbb{S}_0)$.

Also the precision parameter M in Talbot algorithm is set as $M = 20$. The numerical results of different maturities T are given in Table 3.1. As one can see, the contract value behaves as a monotonically increasing function of the maturity time T .

We also compare our results with the upper bound of $V_1(T)|_{a=0}$ as provided in Section 3.4.1 to determine whether our pricing formulas upper bound can be replicated through the use of a lookback option. Table 3.2 provides the results and comparison of our product and the lookback option. As can be seen from the table, the results are identical (actually the numbers are nearly identical up to nearly 12 significant digits).

Now we move to test the sensitivity of each parameter. Figure 3.1 give the sensitivity testing regarding the drawdown size a , risk free rate r and volatility σ . The base parameters are defined as previously for each graph except for the single parameter being tested in each graph respectively.

Figure 3.1 (a) shows us how the price changes based on varying drawdown sizes a . The lower the drawdown size, the more likely a drawdown will occur, so the knock-in condition will be easier reach. As such, the contact value will increase more quickly with a lower maturity time T and begin to slow down as the maturity time increases. As the drawdown size a

T	$V_1(T)$
0.25	0.03966
0.5	0.50447
0.75	1.24232
1	1.99043
1.25	2.67188
1.5	3.27754
1.75	3.81538
2	4.29564
2.25	4.72729
2.5	5.11751
2.75	5.47202
3	5.79540

Table 3.1: The fair market value of Type I knock-in drawdown option $V_1(T)$

T	$V_1(T) _{a=0}$	Lookback Option
0.25	3.44719	3.44719
0.50	4.57750	4.57750
0.75	5.33797	5.33797
1.00	5.91192	5.91192
1.25	6.36986	6.36986
1.50	6.74767	6.74767
1.75	7.06648	7.06648
2.00	7.33995	7.33995
2.25	7.57746	7.57746
2.50	7.78578	7.78578
2.75	7.96994	7.96994
3.00	8.13383	8.13383

Table 3.2: Comparison of $V_1(T)|_{a=0}$ with the lookback option

increases, the price begins to increase more slowly for lower maturity times as the expectation for a drawdown to occur with a small maturity time and higher drawdown size is small. As the maturity increases, the price begins to increase more quickly once again.

From Figure 3.1 (b), we see that the sensitivity with respect to r follows some similar patterns, where the contract value is decreasing in r . Actually, the discount factor e^{-rT} , the payoff P_T , the knock-in condition $1_{\{T_{\frac{\alpha}{\delta}}^+(\alpha) < T\}}$ all depend on both the risk free rate r and maturity time T . For each r the price increasing with maturity but the trend of increasing is getting slower. As the maturity time T increases, the difference between the prices grows larger as r decreasing.

Figure 3.1 (c) shows the sensitivity test for the volatility σ . As expected, the higher the volatility, the higher the contract value. When the volatility is small enough (the black line where $\sigma = 0.05$) we have a very flat price curve around 0, because the probability for a relative

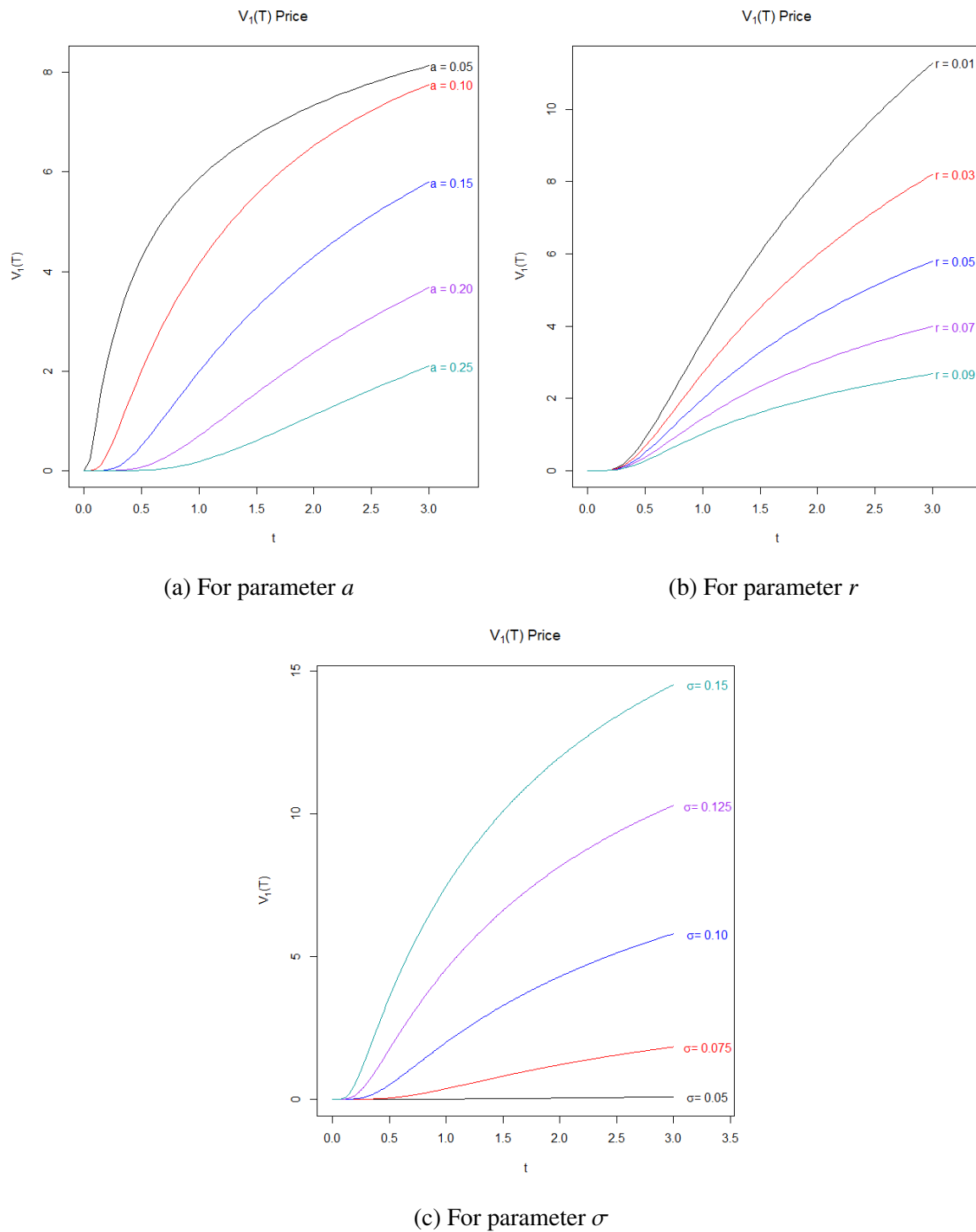


Figure 3.1: Sensitivity tests for Type I knock-in drawdown option $V_1(T)$

drawdown of our specified size $a = 0.15$ becomes very small when the volatility is so low, and the payoff at maturity as the difference of the running maximum and current value will be small as well. On the other end of the spectrum, as the volatility becomes large, the price begins to significantly increase.

3.5.2 Type II option

Numerical LT inversion of results in Theorem 3.3.2 are shown in Table 3.3 with the following parameter setting:

- the risk-free rate $r = 0.05$
- absolute drawdown size $a = 0.15$, or equivalently $\alpha = 1 - e^{-a}$
- the volatility $\sigma = 0.10$

Note that the initial value \mathbb{S}_0 is irrelevant in the Type II option pricing.

T	$V_2(T)$
0.25	0.00329
0.5	0.04223
0.75	0.10556
1	0.17189
1.25	0.23419
1.5	0.29079
1.75	0.34168
2	0.38721
2.25	0.42786
2.5	0.46408
2.75	0.49626
3	0.52478

Table 3.3: The fair market value of Type II knock-in drawdown option $V_2(T)$

When we examine the connection to the digital option on maximum drawdown under Section 3.4.2, by setting $\beta = 0$, we have Figure 3.2 showing the result comparison of our regular Type II payoff (black line $\beta = 1$) to the lower bound (red line $\beta = 0$) as the digital call option on maximum drawdown.

Figure 3.3 shows the sensitivity tests of $V_2(T)$ regarding the drawdown size a , risk free rate r , and the volatility σ . Recall that the valuation is the risk-neutral expectation of three components, i.e., the discount factor e^{-rt} , the payoff $e^{\bar{X}_T - X_T}$, and the knock-in condition $1_{\{\tau_D^+(a) < T\}}$.

Figure 3.3 (a) shows the price changes as a function of maturity T under different values of a . For a fixed maturity time T , the larger the a the smaller the price. This could be explained as the parameters a only affects the knock-in condition: the larger the a , the less likely a knock-in drawdown will happens, hence the lower the price. For a fixed drawdown size a (large enough), we observe a monotone increasing price as the maturity T increases. However, a

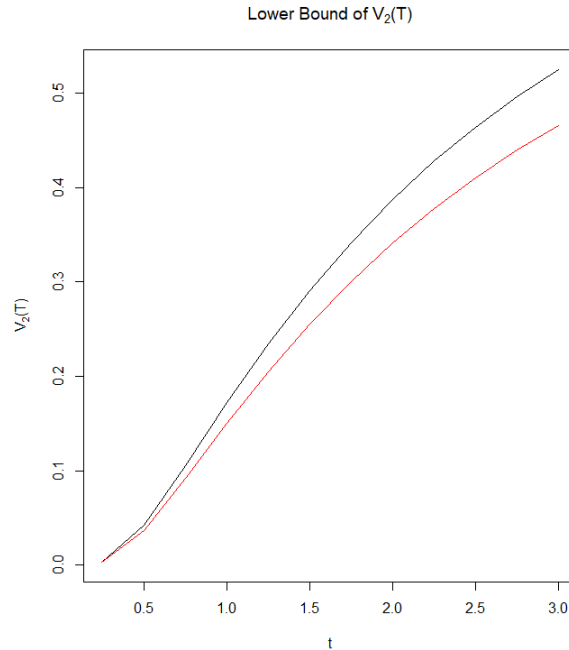
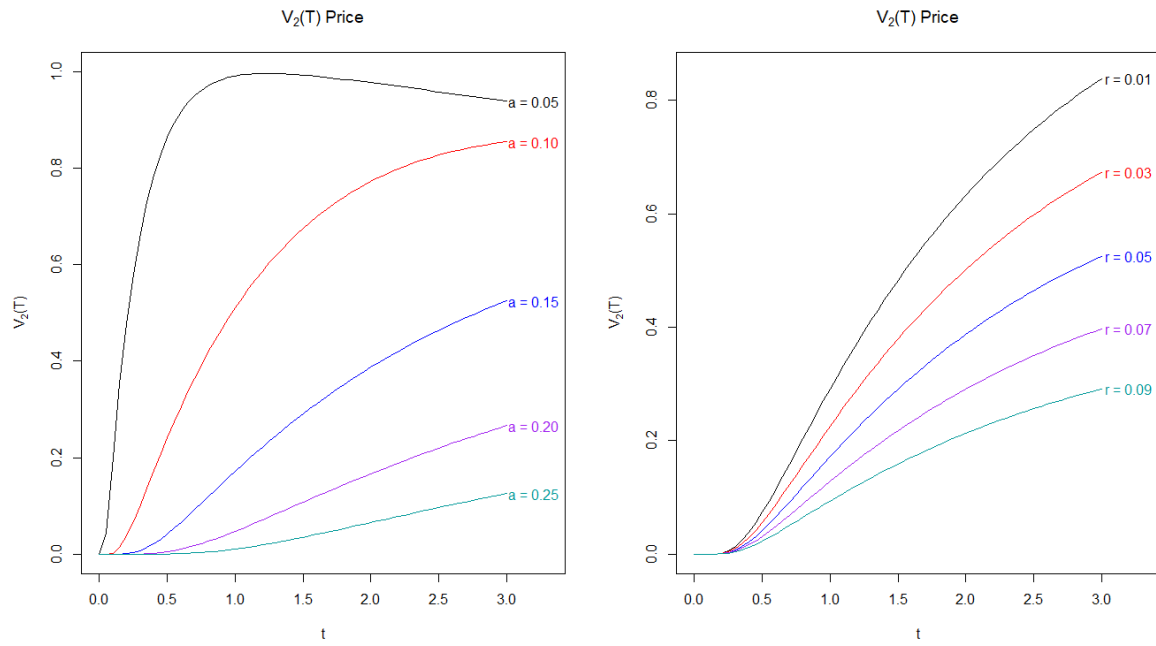


Figure 3.2: The values of $V_2^\beta(T)$ with black representing $\beta = 1$ and red representing $\beta = 0$

different pattern shows when $a = 0.05$, where we have an increase and then decrease in price as maturity increases. This could be explained by the impacts of the maturity time T on the discount factor and the payoff. To better examine which effect is more important to cause the different pattern, we further let the risk free rate $r = 0$ (means no discounting) and plot Figure 3.4. As can be seen in Figure 3.4 (b), when $r = 0$, the price becomes monotone increasing on maturity time T at all drawdown size levels a as expected. On the other hand, we let $\beta = 0$ in $V_2^\beta(T)$ to eliminate the effect on payoff, and find the pattern is similar to Figure 3.4 (a). Hence, we conclude that the reasons for an increase-then-decrease pattern in Figure 3.3 (a) could be mainly explained as follows: when T is small, the knock-in condition plays a dominant role in the valuation, hence the longer the maturity, the higher chance for the option to be knocked-in; however, when T becomes large enough, the discount factor (with $r \neq 0$) plays a dominant role in the valuation, hence the longer the maturity, the smaller the present value.

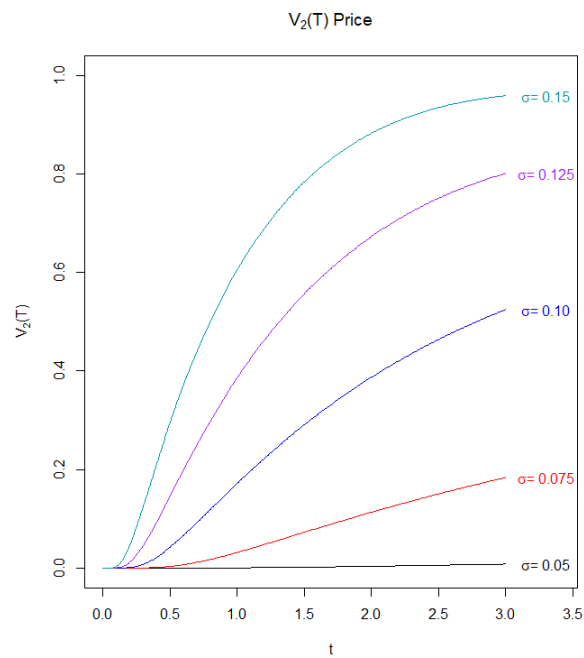
In Figure 3.3 (b), we test sensitivity of the risk free rate r . The graph itself is very similar as in the type I payoff, where the price is higher with lower discounting factor as maturity increases. As maturity T increases, the differences of the prices under different level of risk-free rate become larger as well.

Figure 3.3 (c) illustrates the sensitivity test for the volatility σ . The graph is similar to that in the type I payoff. As expected, the higher the volatility, the higher the option price. When the volatility is small enough (the black line where $\sigma = 0.05$) we have a very flat price curve around 0, because the probability for a relative drawdown of our specified size $a = 0.15$ becomes very small when the volatility is so low, and the payoff at maturity as the difference of the running maximum and current value will be small as well.



(a) For parameter a

(b) For parameter r



(c) For parameter σ

Figure 3.3: Sensitivity tests for Type II knock-in drawdown option $V_2(T)$

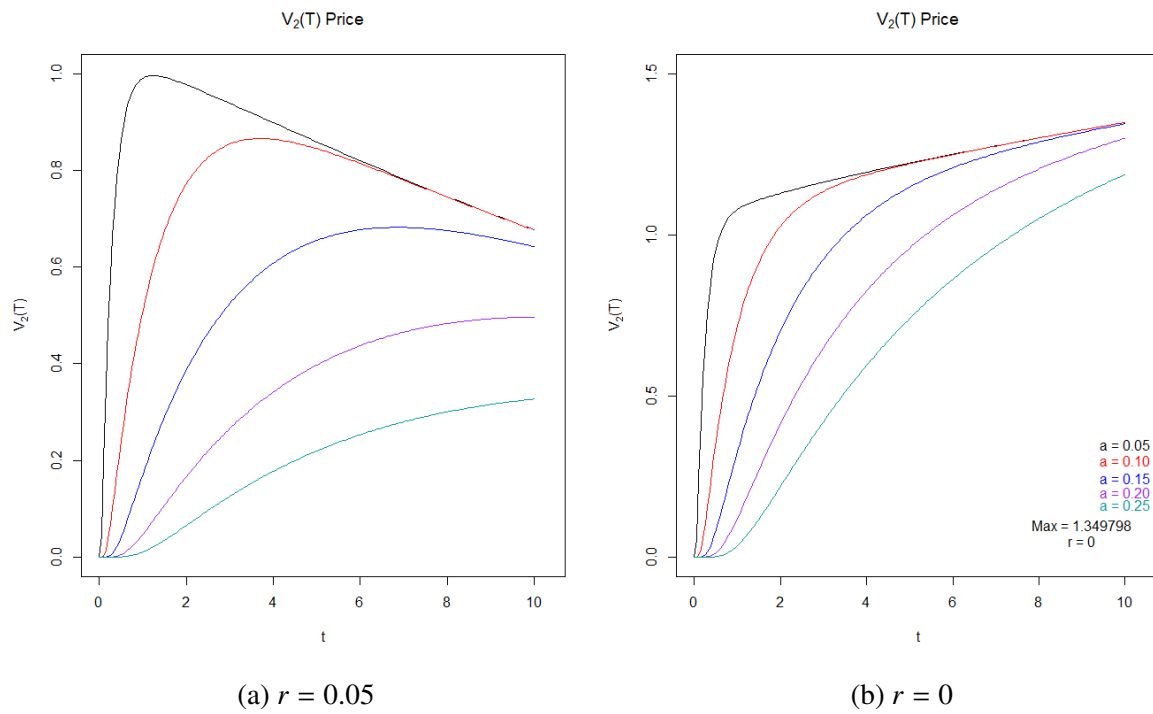


Figure 3.4: Sensitivity test for Type II knock-in drawdown option $V_2(T)$ wrt a

Chapter 4

Conclusion and Future Work

In this thesis, we have designed several insurance and option contracts based on the stochastic drawdowns, which provide protections against the size of drawdowns, the frequency of drawdowns and the speed of market crash. We mainly focus on the fair market valuation of these contracts whose underlying asset follows the dynamic of geometric Brownian motion (i.e., the log-asset is modeled by Brownian motion). Such a Brownian motion setting, as a special case of linear diffusion model and spectrally negative Lévy process, allows us to derive the main results (semi-)explicitly. In particular, we utilize a probabilistic argument to derive the price formulas in terms of their Laplace transforms. Then we compute the numerical Laplace inversion to complete the valuation for the insurance and option products.

In Chapter 2, we design a drawdown insurance contract whose claim depends on the number of market crashes before maturity. Actually, there are four contracts discussed in details, depending on the with/without recovery case

$$V(T, b) = e^{-rT} \sum_{n=1}^{\infty} \mathbb{E}(1_{\{\tau_D^{n,+}(a) \leq T, S_a^n < b\}}),$$

$$\tilde{V}(T, b) = e^{-rT} \sum_{n=1}^{\infty} \mathbb{E}(1_{\{\bar{\tau}_D^{n,+}(a) \leq T, \bar{S}_a^n < b\}}),$$

or the claim payment timing and whether there is a knock-out barrier

$$V_\tau(T, b) = \sum_{n=1}^{\infty} \mathbb{E}(e^{-r\tau_D^{n,+}(a)} 1_{\{\tau_D^{n,+}(a) \leq T, S_a^n < b\}}),$$

$$V_B(T, b) = e^{-rT} \sum_{n=1}^{\infty} \mathbb{E}_x(1_{\{\tau_D^{n,+}(a) \leq T, S_a^n < b, X_{g_a^n} < B\}}).$$

And we could similarly generalize the last two types to the with recovery case. Numerical examples and sensitivity tests are then conducted for $V(T, b)$ and $\tilde{V}(T, b)$ using the two-dimensional Laplace inversion.

In Chapter 3, we propose a knock-in drawdown option, where the knock-in feature depends on the maximum (proportional) drawdown before maturity. We discuss three contracts with different payoff functions

$$V_1(T) = \mathbb{E}\left[e^{-rT} (\bar{S}_T - S_T) 1_{\{T_S^+(a) < T\}}\right],$$

$$V_2(T) = \mathbb{E}\left[e^{-rT} \left(\frac{\bar{S}_T}{S_T}\right) 1_{\{T_S^+(\alpha) < T\}}\right],$$

and a more general

$$V_2^\beta(T) = \mathbb{E}\left[e^{-rT} \left(\frac{\bar{S}_T}{S_T}\right)^\beta 1_{\{T_S^+(\alpha) < T\}}\right].$$

We examine the connections with existing models, where the lookback put option is an upper bound for $V_1(T)$ and digital option on maximum drawdown is a lower bound for $V_2^\beta(T)$. We then present numerical examples and sensitivity tests using the one-dimensional Laplace inversion.

There are several directions that we would like to continue to explore in the future work. First, we would like to examine other numerical Laplace inversion methods and their accuracy. Even though the Talbot methods used in this thesis already provide the accurate results, other methods mentioned in the paper and how effectively they could be used especially in two-dimensional case could be explored. Second, new insurance products can be designed using drawdowns, as the flexibility of these contracts was demonstrated in this thesis. On top of this, replication and hedging is a field which can be further explored and should be, as to show how the investors could adopt the risk management strategies on these innovative products. Also, more details are needed to explain how the drawdown insurance/options provided can help protect investors. For example, does the purchase of drawdown insurance/options help to reduce the ruin probability or earn more profit? Finally, we hope to be able to complete the lower bound for the type II payoff in Chapter 3, i.e., the digital option on maximum drawdown explicitly, as to show the consistency of this pricing formula to an existing model. The reason why the lower bound was left out was due to the complexity. As can be seen from Theorem 7.8 in [18], there is a complicated formula that can be used to solve for it using the replication method. However, the provided formula uses bonds, one-touch options, lookback put and call options as well as summations of integrals of options to price. Hence, we will leave this to future works as this thesis has focused on the pricing aspect of these new products.

Bibliography

- [1] Abate, J.; Whitt, W.; A unified framework for numerically inverting Laplace transforms. *INFORMS Journal on Computing* 18, pp. 408–421, 2006.
- [2] Ben-Salah, Z.; Gu’erin, H.; Morales, M.; Firouzi, H. O. On the depletion problem for an insurance risk process: new non-ruin quantities in collective risk theory. *European Actuarial Journal*, 2015.
- [3] Carr, P.; Zhang, H.; Hadjiliadis, O. Maximum drawdown insurance. *International Journal of Theoretical and Applied Finance*, 14(8), pp. 1195-1230, 2011.
- [4] Chesney, M.; Jeanblanc, M; Yor, M. Brownian excursions and Parisian barrier options. *Advances in Applied Probability* 29, pp. 165–184, 1997.
- [5] Dickson D. On the distribution of the surplus prior to ruin. *Insurance: Mathematics and Economics*, Volume 11(3), pp.191-207, 1992.
- [6] Douady, R.; Shiryaev, A.; Yor, M. On probability characteristics of “downfalls” in a standard Brownian motion. *Theory of Probability and Its Applications*, 44(1), pp. 29-38, 2000.
- [7] Gerber, H.; Shiu E. On the Time Value of Ruin. *North American Actuarial Journal*, 2, pp. 48-72, 1998.
- [8] Kuznetsov, A.; Kyprianou, A. E; Rivero, V. The theory of scale functions for spectrally negative Lévy processes. *Springer Lecture Notes in Mathematics* 2061, pp. 1-91, 2013.
- [9] Kyprianou, A. *Fluctuations of Lévy Processes with Applications*. Springer-Verlag Berlin Heidelberg, 2014.
- [10] Landriault, D., Li, B., Li, S. Analysis of a Drawdown-Based Regime-Switching Levy Insurance Model. *Insurance: Mathematics and Economics*, 60, pp. 98-107, 2015.
- [11] Landriault, D., Li, B., Li, S. Expected Utility of the Drawdown-Based Regime-Switching Risk Model with State-Dependent Termination. *Insurance: Mathematics and Economics*, 79, pp. 137-147, 2018.
- [12] Landriault, D.; Li, B.; Zhang, H. On the frequency of drawdowns for Brownian motion processes. *Journal of Applied Probability*, 52, pp. 191-208, 2015.

- [13] Magdon-Ismail, M.; Atiya, A.; Pratap, A.; Abu-Mostafa, Y. On the maximum drawdown of a Brownian motion. *Journal of Applied Probability*, 41, pp. 147-161, 2004.
- [14] Mendes. B.; Leal R. Maximum Drawdown: Models and Applications. *Coppead Working Paper Series No. 359*, 2004. SSRN: https://papers.ssrn.com/sol3/papers.cfm?abstract_id=477322.
- [15] Mijatovic, A.; Pistorius, M. On the drawdown of completely asymmetric Lévy processes. *Stochastic Processes and their Applications*, 122(11), 3812-3836, 2012.
- [16] Taylor, H. A stopped Brownian motion formula. *Annals of Probability*, 3(2), pp. 234-246, 1975.
- [17] Zhang, H. Drawdowns, Drawups and Their Applications. Doctoral Thesis, City University of New York, 2010.
- [18] Zhang, H. *Stochastic Drawdowns*. World Scientific, Volume 2, 2018.

Appendix A

Proof of Equation (3.18)

Proof Recall that the risk free rate r has the relationship $r = \mu + \frac{\sigma^2}{2}$, and it is possible for $r > \frac{\sigma^2}{2}$ or $r < \frac{\sigma^2}{2}$.

When $\bar{\mathbb{S}}_0 = \mathbb{S}_0 = S$, we have

$$\begin{aligned}
 \hat{V}_u(T) &= S e^{-rT} N(-d_1 + \sigma \sqrt{T}) - S N(-d_1) + \frac{\sigma^2}{2r} S \left(N(d_1) - e^{-rT} N(d_1 - \frac{2r}{\sigma} \sqrt{T}) \right) \\
 &= S \left(e^{-rT} N(-d_1 + \sigma \sqrt{T}) - N(-d_1) + \frac{\sigma^2}{2r} N(d_1) - \frac{\sigma^2}{2r} e^{-rT} N(d_1 - \frac{2r}{\sigma} \sqrt{T}) \right) \\
 &= S \left(e^{-rT} N(-d_2) - N(-d_1) + \frac{\sigma^2}{2r} N(d_1) - \frac{\sigma^2}{2r} e^{-rT} N(-d_2) \right) \\
 &= S \left(e^{-rT} \left(1 - \frac{\sigma^2}{2r}\right) N(-d_2) + \left(1 + \frac{\sigma^2}{2r}\right) N(d_1) - 1 \right),
 \end{aligned}$$

with

$$d_1 = \frac{(r + \sigma^2/2)T}{\sigma \sqrt{T}}, \quad N(-d_1) = 1 - N(d_1),$$

and

$$d_2 := d_1 - \sigma \sqrt{T} = -(d_1 - \frac{2r}{\sigma} \sqrt{T}) = \frac{(r - \sigma^2/2)T}{\sigma \sqrt{T}}.$$

Hence, taking the LT with respect to T on $\hat{V}_u(T)$, we have

$$\begin{aligned}
 \int_0^\infty e^{-qT} \hat{V}_u(T) dT &= S \int_0^\infty e^{-qT} \left(e^{-rT} \left(1 - \frac{\sigma^2}{2r}\right) N(-d_2) + \left(1 + \frac{\sigma^2}{2r}\right) N(d_1) - 1 \right) dT \\
 &= S \left(1 - \frac{\sigma^2}{2r}\right) \int_0^\infty e^{-(q+r)T} N(-d_2) dT + S \left(1 + \frac{\sigma^2}{2r}\right) \int_0^\infty e^{-qT} N(d_1) dT - S \int_0^\infty e^{-qT} dT,
 \end{aligned}$$

where

$$\int_0^\infty e^{-qT} dT = \frac{1}{q}.$$

Denoting $d_1 := D_1 \sqrt{T}$ with $D_1 = \frac{r+\sigma^2/2}{\sigma} > 0$ and using the (standard) normal density $f(x) = \frac{1}{\sqrt{2\pi}} e^{-\frac{1}{2}x^2}$ (with mean 0 and variance 1), we have

$$\begin{aligned}
\int_0^\infty e^{-qT} N(d_1) dT &= \int_0^\infty e^{-qT} \int_{-\infty}^{d_1} \frac{1}{\sqrt{2\pi}} e^{-\frac{1}{2}x^2} dx dT \\
&= \int_0^\infty e^{-qT} \left(\int_{-\infty}^0 \frac{1}{\sqrt{2\pi}} e^{-\frac{1}{2}x^2} dx + \int_0^{D_1 \sqrt{T}} \frac{1}{\sqrt{2\pi}} e^{-\frac{1}{2}x^2} dx \right) dT \\
&= \int_{-\infty}^0 \frac{1}{\sqrt{2\pi}} e^{-\frac{1}{2}x^2} \int_0^\infty e^{-qT} dT dx + \int_0^\infty \frac{1}{\sqrt{2\pi}} e^{-\frac{1}{2}x^2} \int_{x^2/D_1^2}^\infty e^{-qT} dT dx \\
&= \int_{-\infty}^0 \frac{1}{\sqrt{2\pi}} e^{-\frac{1}{2}x^2} \frac{1}{q} dx + \int_0^\infty \frac{1}{\sqrt{2\pi}} e^{-\frac{1}{2}x^2} \frac{e^{-q \frac{x^2}{D_1^2}}}{q} dx \\
&= \frac{1}{q} \cdot \frac{1}{2} + \frac{1}{q} \int_0^\infty \frac{1}{\sqrt{2\pi}} e^{-\left(\frac{1}{2} + \frac{q}{D_1^2}\right)x^2} dx \\
&= \frac{1}{2q} + \frac{1}{q} \frac{D_1}{\sqrt{D_1^2 + 2q}} \int_0^\infty \frac{1}{\sqrt{2\pi}} e^{-\frac{1}{2}y^2} dy \\
&= \frac{1}{2q} \left(1 + \frac{D_1}{\sqrt{D_1^2 + 2q}} \right) = \frac{1}{2q} \left(1 + \frac{r + \sigma^2/2}{\sqrt{(r + \sigma^2/2)^2 + 2q\sigma^2}} \right).
\end{aligned}$$

And similarly, letting $d_2 := D_2 \sqrt{T}$ with $D_2 = \frac{r-\sigma^2/2}{\sigma}$. Assuming $D_2 > 0$, we have

$$\begin{aligned}
\int_0^\infty e^{-(q+r)T} N(-d_2) dT &= \int_0^\infty e^{-(q+r)T} \int_{-\infty}^{-d_2} \frac{1}{\sqrt{2\pi}} e^{-\frac{1}{2}x^2} dx dT \\
&= \int_{-\infty}^0 \frac{1}{\sqrt{2\pi}} e^{-\frac{1}{2}x^2} \left(\int_0^{x^2/D_2^2} e^{-(q+r)T} dT \right) dx \\
&= \int_{-\infty}^0 \frac{1}{\sqrt{2\pi}} e^{-\frac{1}{2}x^2} \left(\frac{1 - e^{-\frac{(q+r)x^2}{D_2^2}}}{q+r} \right) dx \\
&= \frac{1}{q+r} \cdot \frac{1}{2} - \frac{1}{q+r} \int_0^\infty \frac{1}{\sqrt{2\pi}} e^{-\left(\frac{1}{2} + \frac{q+r}{D_2^2}\right)x^2} dx \\
&= \frac{1}{2(q+r)} - \frac{1}{q+r} \frac{D_2}{\sqrt{D_2^2 + 2(q+r)}} \int_0^\infty \frac{1}{\sqrt{2\pi}} e^{-\frac{1}{2}y^2} dy \\
&= \frac{1}{2(q+r)} \left(1 - \frac{D_2}{\sqrt{D_2^2 + 2(q+r)}} \right) = \frac{1}{2(q+r)} \left(1 - \frac{r - \sigma^2/2}{\sqrt{(r - \sigma^2/2)^2 + 2(q+r)\sigma^2}} \right),
\end{aligned}$$

and one can easily verify that the above equation holds for the case of $D_2 < 0$. Actually, when

we have $D_2 < 0$ then $d_2 < 0$ and so $-d_2 > 0$. As such, we have the following

$$\begin{aligned}
\int_0^\infty e^{-(q+r)T} N(-d_2) dT &= \int_0^\infty e^{-(q+r)T} \int_{-\infty}^{-d_2} \frac{1}{\sqrt{2\pi}} e^{-\frac{1}{2}x^2} dx dT \\
&= \int_0^\infty e^{-(q+r)T} \int_{-\infty}^{-D_2 \sqrt{T}} \frac{1}{\sqrt{2\pi}} e^{-\frac{1}{2}x^2} dx dT \\
&= \int_0^\infty e^{-(q+r)T} \left(\int_{-\infty}^0 \frac{1}{\sqrt{2\pi}} e^{-\frac{1}{2}x^2} dx + \int_0^{-D_2 \sqrt{T}} \frac{1}{\sqrt{2\pi}} e^{-\frac{1}{2}x^2} dx \right) dT \\
&= \int_0^\infty e^{-(q+r)T} \int_{-\infty}^0 \frac{1}{\sqrt{2\pi}} e^{-\frac{1}{2}x^2} dx dT + \int_0^\infty e^{-(q+r)T} \int_0^{-D_2 \sqrt{T}} \frac{1}{\sqrt{2\pi}} e^{-\frac{1}{2}x^2} dx dT \\
&= \frac{1}{q+r} \cdot \frac{1}{2} + \int_0^\infty \frac{1}{\sqrt{2\pi}} e^{-\frac{1}{2}x^2} \int_{x^2/D_2^2}^\infty e^{-(q+r)T} dT dx \\
&= \frac{1}{q+r} \cdot \frac{1}{2} + \frac{1}{q+r} \int_0^\infty \frac{1}{\sqrt{2\pi}} e^{-\left(\frac{1}{2} + \frac{q+r}{D_2^2}\right)x^2} dx \\
&= \frac{1}{q+r} \cdot \frac{1}{2} + \frac{1}{q+r} \cdot \frac{-D_2}{\sqrt{D_2^2 + 2(q+r)}} \int_0^\infty \frac{1}{\sqrt{2\pi}} e^{-\frac{1}{2}y} dy \\
&= \frac{1}{2(q+r)} - \frac{1}{q+r} \frac{D_2}{\sqrt{D_2^2 + 2(q+r)}} \cdot \frac{1}{2} \\
&= \frac{1}{2(q+r)} \left(1 - \frac{r - \sigma^2/2}{\sqrt{(r - \sigma^2/2)^2 + 2(q+r)\sigma^2}} \right).
\end{aligned}$$

Therefore, putting all together and recall that $\phi(q+r) = \frac{-(r - \sigma^2/2) + \sqrt{(r - \sigma^2/2)^2 + 2(q+r)\sigma^2}}{\sigma^2}$, one has

$$\begin{aligned}
&\int_0^\infty e^{-qT} \hat{V}_u(T) dT \\
&= S \left(1 - \frac{\sigma^2}{2r} \right) \frac{1}{2(q+r)} \left(1 - \frac{r - \sigma^2/2}{\sqrt{(r - \sigma^2/2)^2 + 2(q+r)\sigma^2}} \right) + S \left(1 + \frac{\sigma^2}{2r} \right) \frac{1}{2q} \left(1 + \frac{r + \sigma^2/2}{\sqrt{(r + \sigma^2/2)^2 + 2q\sigma^2}} \right) - S/q,
\end{aligned}$$

And as the last step, we can show the following equation holds (via the LHS minus the RHS equals zero)

$$\begin{aligned}
&\left(1 - \frac{\sigma^2}{2r} \right) \frac{1}{2(q+r)} \left(1 - \frac{r - \sigma^2/2}{\sqrt{(r - \sigma^2/2)^2 + 2(q+r)\sigma^2}} \right) + \left(1 + \frac{\sigma^2}{2r} \right) \frac{1}{2q} \left(1 + \frac{r + \sigma^2/2}{\sqrt{(r + \sigma^2/2)^2 + 2q\sigma^2}} \right) \\
&= \frac{1}{q+r} \frac{\phi(q+r)}{\phi(q+r) - 1}.
\end{aligned}$$

Therefore, matching the expressions, we have

$$\int_0^\infty e^{-qT} \hat{V}_u(T) dT = \int_0^\infty e^{-qT} V_u(T) dT.$$

Appendix B

Proof of Equation (3.20)

Proof The proof of this theorem can be done in a similar way as Theorem 3.3.1 by separating the expectation into $DDP^{(1)}$ and $DDP^{(2)}$, depending on whether e_q happens before or after recovery. However, we need to incorporate the new payoff for this Type II product. Similarly we could consider the LT of $V_2^\beta(T)$ and recall Equation (3.13) that

$$\begin{aligned} q \int_0^\infty e^{-qT} V_2^\beta(T) dT &= \mathbb{E}_x \left[e^{-re_q} P_{e_q}^\beta \mathbf{1}_{\{\tau_D^+(a) < e_q\}} \right] \\ &= \mathbb{E}_x \left(e^{-re_q} P_{e_q}^\beta \cdot \mathbf{1}_{\{\tau_D^+(a) < e_q, T_1 < e_q\}} \right) + \mathbb{E}_x \left(e^{-re_q} P_{e_q}^\beta \cdot \mathbf{1}_{\{\tau_D^+(a) < e_q, T_1 > e_q\}} \right) \\ &:= DDP^{(1)} + DDP^{(2)}, \end{aligned}$$

where with the type II payoff function is given as $P_t^\beta = e^{\beta(\bar{X}_t - X_t)}$.

By conditioning on the drawdown time and the running maximum before drawdown, we make use of the strong Markov property of X and it gives

$$\begin{aligned} DDP^{(1)} &= \int_x^\infty \mathbb{E}_x \left(e^{-(r+q)\tau_D^+(a)} \cdot \mathbf{1}_{\{\bar{X}_{\tau_D^+(a)} \in dy\}} \right) \cdot \mathbb{E}_{y-a} \left(e^{-(r+q)\tau_X^+(y)} \right) \cdot \mathbb{E}_y \left(e^{-re_q} P_{e_q}^\beta \right) \\ &= \frac{C^{(q+r)}(a)}{\rho^{(q+r)}(a)} e^{-\phi(q+r)a} \frac{q}{\phi(q+r)} \frac{\phi(q+r) + \beta}{q+r - \psi(-\beta)}, \end{aligned}$$

where we have

$$\mathbb{E}_y \left(e^{-re_q} P_{e_q}^\beta \right) = \mathbb{E}_y \left(e^{-re_q} e^{\beta(\bar{X}_{e_q} - X_{e_q})} \right) = \frac{q}{\phi(q+r)} \frac{\phi(q+r) + \beta}{q+r - \psi(-\beta)},$$

using Equations (3.7). This completes the calculation for $DDP^{(1)}$.

Now we move to $DDP^{(2)}$. If the running maximum is not recovered, by conditioning on the drawdown time and the running maximum before drawdown, we have

$$\begin{aligned} DDP^{(2)} &= \int_x^\infty \mathbb{E}_x \left(e^{-(r+q)\tau_D^+(a)} \cdot \mathbf{1}_{\{\bar{X}_{\tau_D^+(a)} \in dy\}} \right) \cdot \mathbb{E}_{y-a} \left(e^{-re_q} P_{e_q}^\beta \cdot \mathbf{1}_{\{\tau_X^+(y) > e_q\}} \right) \\ &= \int_x^\infty \mathbb{E}_x \left(e^{-(r+q)\tau_D^+(a)} \cdot \mathbf{1}_{\{\bar{X}_{\tau_D^+(a)} \in dy\}} \right) \cdot \mathbb{E}_{y-a} \left(e^{-re_q} (e^{\beta(y - X_{e_q})}) \cdot \mathbf{1}_{\{\tau_X^+(y) > e_q\}} \right), \end{aligned}$$

where the second part in the integration can be calculated as

$$\begin{aligned}
& \mathbb{E}_{y-a} \left(e^{-re_q} (e^{\beta y - \beta X_{e_q}}) \cdot \mathbf{1}_{\{\tau_X^+(y) > e_q\}} \right) \\
&= \mathbb{E}_0 \left(e^{-re_q} (e^{\beta a - \beta X_{e_q}}) \cdot \mathbf{1}_{\{\tau_X^+(a) > e_q\}} \right) \\
&= e^{\beta a} \left(\mathbb{E}_0 \left(e^{-re_q} e^{-\beta X_{e_q}} \right) - \mathbb{E}_0 \left(e^{-re_q} e^{-\beta X_{e_q}} \cdot \mathbf{1}_{\{\tau_X^+(a) < e_q\}} \right) \right) \\
&= e^{\beta a} \left(\frac{q}{q+r-\psi(-\beta)} - e^{-\phi(q+r)a} e^{-\beta a} \frac{q}{q+r-\psi(-\beta)} \right) \\
&= \frac{q}{q+r-\psi(-\beta)} \left(e^{\beta a} - e^{-\phi(q+r)a} \right),
\end{aligned}$$

using Equation (3.6).

Thus, substituting this back to the $DDP^{(2)}$ and together with Lemma 3.2.1, we have

$$\begin{aligned}
DDP^{(2)} &= \int_x^\infty C^{(q+r)}(a) e^{-\rho^{(q+r)}(a)(y-x)} \frac{q}{q+r-\psi(-\beta)} \left(e^{\beta a} - e^{-\phi(q+r)a} \right) dy \\
&= \frac{C^{(q+r)}(a)}{\rho^{(q+r)}(a)} \frac{q}{q+r-\psi(-\beta)} \left(e^{\beta a} - e^{-\phi(q+r)a} \right).
\end{aligned}$$

Finally, by adding $DDP^{(1)}$ and $DDP^{(2)}$ together,

$$\begin{aligned}
& q \int_0^\infty e^{-qT} V_2(T) dT = DDP^{(1)} + DDP^{(2)} \\
&= \frac{C^{(q+r)}(a)}{\rho^{(q+r)}(a)} e^{-\phi(q+r)a} \frac{q}{\phi(q+r)} \frac{\phi(q+r) + \beta}{q+r-\psi(-\beta)} + \frac{C^{(q+r)}(a)}{\rho^{(q+r)}(a)} \frac{q}{q+r-\psi(-\beta)} \left(e^{\beta a} - e^{-\phi(q+r)a} \right) \\
&= \frac{q}{q+r-\psi(-\beta)} \frac{C^{(q+r)}(a)}{\rho^{(q+r)}(a)} \left[e^{\beta a} + \frac{\beta}{\phi(q+r)} e^{-\phi(q+r)a} \right],
\end{aligned}$$

which completes the proof.

Curriculum Vitae

Name: Filip Dikic

Post-Secondary Education and Degrees: University of Western Ontario
London, ON
2018 - Present M.S.c candidate

University of Western Ontario
London, ON
2014 - 2018 B.Sc.

Related Work Experience: Teaching Assistant
The University of Western Ontario
2018 - 2020